

## BACHELOR THESIS

# Modelling of the magnetic states and phase transitions in hematite

**Author**  
Bennet Karetta

**Supervisor**  
Dr. Olena Gomonyay

INSPIRE  
Faculty 08 - Institute for physics  
Johannes Gutenberg-Universität Mainz

### Abstract

We minimize the anisotropy energy in the antiferromagnet hematite ( $\alpha$ -Fe<sub>2</sub>O<sub>3</sub>) with respect to its magnetization and Néel vector. Using analytical methods, we search for stable states in the anisotropy, that we get from its minima, to obtain the behaviour of the Néel vector for different situations of external magnetic fields. Furthermore, we check the results by also numerically finding the stable magnetic states in hematite and determining its spin hall magnetoresistance. From this we set up a phase diagram for the magnetic ordering in hematite in the easy axis phase in relation to an external magnetic field.



Mainz, February 13, 2019

Ich versichere, dass ich die Arbeit "Modelling of the magnetic states and phase transitions in hematite" selbstständig verfasst und keine anderen als die in der Arbeit angegebenen Quellen und Hilfsmittel benutzt sowie Zitate kenntlich gemacht habe.

I assure, that I have written the thesis "Modelling of the magnetic states and phase transitions in hematite" by myself and that I have not used or cited sources different to the ones given in the thesis.

Mainz, den 13.02.2019  
Bennet Karetta

# Contents

|   |           |
|---|-----------|
| <b>1. Introduction</b>  | <b>1</b>  |
| <b>2. Analysis of the anisotropy in hematite</b>                        | <b>2</b>  |
| 2.1. Notation . . . . .   | 2         |
| 2.2. Minimizing $w_{ani}$ with respect to $\vec{m}$ . . . . .           | 3         |
| 2.3. Minimizing $w_{ani}$ with respect to $\vec{n}$ . . . . .           | 4         |
| 2.4. Field free case . . . . .  | 6         |
| 2.5. Uniaxial anisotropy . . . . .                                      | 7         |
| 2.5.1. Magnetic field parallel to the easy plane . . . . .              | 7         |
| 2.5.2. Magnetic field parallel to the easy axis . . . . .               | 9         |
| 2.5.3. Arbitrary magnetic field . . . . .                               | 10        |
| 2.5.4. Brief summary of the results . . . . .                           | 12        |
| 2.6. General anisotropy . . . . .                                       | 13        |
| 2.6.1. Magnetic field parallel to the easy plane . . . . .              | 13        |
| 2.6.2. Magnetic field parallel to the easy axis . . . . .               | 14        |
| 2.6.3. Arbitrary magnetic field . . . . .                               | 15        |
| <b>3. Numerical investigation of the anisotropy in easy axis phase</b>  | <b>17</b> |
| 3.1. Analysing method . . . . .   | 17        |
| 3.2. One dimensional scans . . . . .                                    | 18        |
| 3.2.1. Scan with fixed field orientation . . . . .                      | 19        |
| 3.2.2. Scan with fixed field strength . . . . .                         | 20        |
| 3.3. Two dimensional scan . . . . .                                     | 22        |
| 3.4. Phase diagrams . . . . .   | 24        |
| <b>4. Numerical investigation of the anisotropy in easy plane phase</b> | <b>26</b> |
| <b>5. Conclusion</b>  | <b>29</b> |
| <b>A. Appendix</b>  | <b>31</b> |
| A.1. Additional plots for the scans in the easy axis phase . . . . .    | 31        |
| A.2. Additional plots for the scans in the easy plane phase . . . . .   | 34        |

# 1. Introduction

The magnetic structure of a material depends on the alignment of the electron spins inside the material [1]. In ferromagnets for example the electrons align their spins all in the same direction for a long range, inducing a net magnetization [2]. Magnetic fields can disturb and turn this magnetization in other directions, due to the interaction of the field and the magnetization. Therefore, spin based electronics or also called spintronics of ferromagnets are very unstable under strong disturbing magnetic fields. For this reason, other materials are investigated on their magnetic structure and especially antiferromagnets are a matter of interest in this research [3, 4] and are a good candidate for new spin based information systems [5].

The spins in antiferromagnetic materials align antiparallel to their neighbours creating two magnetic sublattices  $A$  and  $B$  with opposite magnetization [6]. As for ferromagnets the ordering vanishes after a certain temperature [6], which we call Néel-temperature ( $T_N$ ) for antiferromagnets. Due to the magnetic ordering, antiferromagnets should have no net magnetization, so the material gets less influenced by magnetic fields. Somehow, there is still an influence of the magnetic field on the antiferromagnetic ordering [7], which will be investigated in this thesis.

The focus of this work will be on hematite ( $\alpha$ -Fe<sub>2</sub>O<sub>3</sub>), which is a room temperature antiferromagnet ( $T_N = 675$  °C [8]). The main goal is to achieve the relation of the magnetic ordering inside of hematite in dependence of an external magnetic field. In sec. 2 we will search stable states of the magnetic ordering in hematite with analytical methods. Therefore we will minimize the part of the energy of hematite which has a contribution to the magnetic ordering (Sec. 2.2 and 2.3) from where we can obtain the stable states. We begin without external fields in sec. 2.4 to then see the changes of the magnetic ordering if an magnetic field is applied first in a simplified (Sec. 2.5) and then a more general (Sec. 2.6) model.

Afterwards in sec. 3 we will also do a numerical approach in the easy axis phase to the same problem with the goal to test the results from the previous section. For this we drive with different magnetic fields or orientations through the energy expression of hematite searching the minima depending on the external field first with only one changing value in sec. 3.2 and afterwards with both field strength and direction in sec. 3.3. Finally in sec 3.4 we will draw a phase diagram of the magnetic ordering in dependence of the external field to summarize the results of this section. In 4 we will test the analytical results with the same method again but for the easy plane phase.

## 2. Analysis of the anisotropy in hematite

### 2.1. Notation

The spins in an antiferromagnet are aligned parallel to a certain axis. To describe this the Néel-vector  $\vec{n}$  is introduced and we define it over  $\vec{n} := (\vec{M}_A - \vec{M}_B)/2M_s$ , where  $\vec{M}_A$  and  $\vec{M}_B$  are the magnetizations of the sublattices  $A$  and  $B$  and  $|\vec{M}_A| = |\vec{M}_B| =: M_s$ . The magnetizations of both sublattices are not always aligned in a perfect antiparallel way due to perturbations or dynamics, therefore a small net magnetization  $\vec{m} := (\vec{M}_A + \vec{M}_B)/2M_s$  will occur in the material. From the definitions of  $\vec{n}$  and  $\vec{m}$  we can obtain a normalization and orthogonality relation

$$\vec{n}^2 + \vec{m}^2 = 1 \quad (2.1)$$

$$\vec{n} \cdot \vec{m} = 0. \quad (2.2)$$

Since  $\vec{M}_A$  and  $\vec{M}_B$  are still almost antiparallel in an antiferromagnet we can assume  $\vec{m}^2 \ll \vec{n}^2$  [9].

It was observed that there is a magnetic anisotropy in hematite [10], that highlights a certain axis in the crystal [11]. We call this axis the easy axis with the easy plane perpendicular to it. Therefore, antiferromagnets have an anisotropy part in their energy, which depends on  $\vec{n}$  and  $\vec{m}$ .

If we choose our coordinate system so that the easy axis is equivalent to the z-axis, the anisotropy energy of hematite under an external magnetic field  $\vec{H}$  has the following form

$$w_{ani} = 2M_s \left[ \frac{H_{ex}}{2} \vec{m}^2 + \frac{H_{2\parallel}}{2} n_z^2 - \frac{H_{\perp}}{6} (n_x^2 - n_y^2) (4(n_x^2 - n_y^2)^2 - 3(n_x^2 + n_y^2)^2) + H_{DMI} (m_x n_y - m_y n_x) - \vec{H} \cdot \vec{m} \right]. \quad (2.3)$$

Here  $H_{ex}$  describes the exchange field in hematite which hold the spins of the sublattices antiparallel.  $H_{2\parallel}$  is the uniaxial anisotropy field and  $H_{\perp}$  is the in-plane anisotropy field. They occur from the crystal symmetry. The Dzyaloshinskii-Moriya field ( $DMI$ -field) is labelled with  $H_{DMI}$  [12]. The values for the fields were previously estimated [13–16] and from that we take  $H_{ex} \gg H_{DMI} \gg |H_{2\parallel}| \gg H_{\perp}$ . We will not use explicit values for these fields in this chapter because they are not constant but depend on temperature,  $H_{2\parallel}$  even flips its sign at a certain temperature called the

Morin temperature [17]. Therefore,  $H_{2\parallel}$  can have a positive or negative sign while the other fields are all estimated to be positive.

## 2.2. Minimizing $w_{ani}$ with respect to $\vec{m}$

The goal is to find stable states for  $\vec{n}$  in the crystal. Therefore, we want to find an expression for  $\vec{m}$  that minimizes  $w_{ani}$ . For that we use the Lagrangian multipliers on the orthogonality condition in eq. 2.2, meaning there is a  $\lambda$ , that fulfils

$$\lambda \nabla_m(\vec{n} \cdot \vec{m}) = \nabla_m w_{ani}.$$

By applying  $\nabla_m$  on the energy expression the relation becomes

$$\begin{aligned} \lambda \vec{n} &= \frac{H_{ex}}{2} 2\vec{m} + H_{DMI} \begin{pmatrix} n_y \\ n_x \\ 0 \end{pmatrix} - \vec{H} \\ \Rightarrow \vec{m} &= \frac{1}{H_{ex}} \left( \vec{H} + \vec{H}_{DMI} \times \vec{n} + \lambda \vec{n} \right) \end{aligned}$$

where  $\vec{H}_{DMI} := H_{DMI} \vec{e}_z$ . We do now have an expression for  $\vec{m}$  that could be used in  $w_{ani}$  but there is still the unknown value  $\lambda$ . To get rid of it we can use eq. 2.2 again.

$$\begin{aligned} 0 &= \left( \vec{H} + (\vec{H}_{DMI} \times \vec{n}) + \lambda \vec{n} \right) \cdot \vec{n} \\ \Rightarrow &= \vec{H} \cdot \vec{n} + (\vec{H}_{DMI} \times \vec{n}) \cdot \vec{n} + \lambda \vec{n} \cdot \vec{n} \\ \Rightarrow 0 &= \vec{H} \cdot \vec{n} + \lambda \\ \Rightarrow \lambda &= -\vec{H} \cdot \vec{n} \end{aligned}$$

Using the normalization eq. 2.1 which can be approximated as  $\vec{n}^2 = 1$  since  $\vec{n}^2 \gg \vec{m}^2$  we find

$$\vec{H} - (\vec{H} \cdot \vec{n})\vec{n} = \vec{H}(\vec{n} \cdot \vec{n}) - \vec{n}(\vec{H} \cdot \vec{n}) = \vec{n} \times \vec{H} \times \vec{n}$$

where also the "bac-cab" identity was applied. This gives the final expression

$$\vec{m} = \frac{1}{H_{ex}} \left( \vec{n} \times \vec{H} \times \vec{n} + \vec{H}_{DMI} \times \vec{n} \right) \quad (2.4)$$

This expression is plugged in to the parts of  $w_{ani}$ , where  $\vec{m}$  occurs.

$$\begin{aligned}\vec{m}^2 &= \frac{1}{H_{ex}^2} \left[ (\vec{H} \times \vec{n})^2 + 2\vec{n}(\vec{H} \times \vec{H}_{DMI}) + (\vec{H}_{DMI} \times \vec{n})^2 \right] \\ \vec{H} \cdot \vec{m} &= \frac{1}{H_{ex}} \left( (\vec{H} \times \vec{n})^2 + \vec{n}(\vec{H} \times \vec{H}_{DMI}) \right) \\ H_{DMI}(m_x n_y - m_y n_x) &= -(\vec{H}_{DMI} \times \vec{n})^2 - \vec{n}(\vec{H} \times \vec{H}_{DMI})\end{aligned}$$

Applying the new relation for  $\vec{m}$  on the anisotropy energy the result is

$$\begin{aligned}w_{ani} &= 2M_s \left[ \frac{H_{ex}}{2} \vec{m}^2 + \frac{H_{2\parallel}}{2} n_z^2 - \frac{H_{\perp}}{6} (n_x^2 - n_y^2)(4(n_x^2 - n_y^2)^2 - 3(n_x^2 + n_y^2)^2) \right. \\ &\quad \left. - \frac{1}{2H_{ex}} \left( (\vec{H} \times \vec{n})^2 + (\vec{H}_{DMI} \times \vec{n})^2 + 2\vec{n}(\vec{H} \times \vec{H}_{DMI}) \right) \right].\end{aligned}\quad (2.5)$$

This expression can be further minimized with respect to  $\vec{n}$  which will be done in the following section.

### 2.3. Minimizing $w_{ani}$ with respect to $\vec{n}$

Using eq. 2.1 and  $\vec{m}^2 \ll \vec{n}^2$  we define spherical coordinates  $n_x = \sin \theta \cos \phi$ ,  $n_y = \sin \theta \sin \phi$  and  $n_z = \cos \theta$ . This is meaningful because we now only have two instead of three variables, that have to minimize  $w_{ani}$ . Then we get the following relations

$$\begin{aligned}(\vec{H} \times \vec{n})^2 &= \vec{H}^2 - (\vec{H} \cdot \vec{n})^2 = H^2 - (H_x \sin \theta \cos \phi + H_y \sin \theta \sin \phi + H_z \cos \theta)^2 \\ (\vec{H}_{DMI} \times \vec{n})^2 &= \vec{H}_{DMI}^2 - (\vec{H}_{DMI} \cdot \vec{n})^2 = H_{DMI}^2 - H_{DMI}^2 \cos^2 \theta \\ \vec{n} \cdot (\vec{H} \times \vec{H}_{DMI}) &= \vec{n} \cdot \begin{pmatrix} H_y H_{DMI} \\ -H_x H_{DMI} \\ 0 \end{pmatrix} = H_y H_{DMI} \sin \theta \cos \phi - H_x H_{DMI} \sin \theta \sin \phi.\end{aligned}$$

With them the energy formula becomes

$$\begin{aligned}\frac{\omega_{ani}}{2M_s} &= \frac{H_{2\parallel}}{2} \cos^2 \theta - \frac{H_{\perp}}{6} (\sin^2 \theta \cos^2 \phi - \sin^2 \theta \sin^2 \phi)(4(\sin^2 \theta \cos^2 \phi - \sin^2 \theta \sin^2 \phi)^2 - 3(\sin^2 \theta)^2) \\ &\quad - \frac{1}{2H_{ex}} (H^2 + H_{DMI}^2 - (H_x \sin \theta \cos \phi + H_y \sin \theta \sin \phi + H_z \cos \theta)^2 - H_{DMI}^2 \cos^2 \theta \\ &\quad + H_y H_{DMI} \sin \theta \cos \phi - H_x H_{DMI} \sin \theta \sin \phi)\end{aligned}\quad (2.6)$$

This equation can still be simplified by using trigonometric relations.

$$\begin{aligned}
& (\sin^2 \theta \cos^2 \phi - \sin^2 \theta \sin^2 \phi)(4(\sin^2 \theta \cos^2 \phi - \sin^2 \theta \sin^2 \phi)^2 - 3(\sin^2 \theta)^2) \\
&= \sin^6 \theta \cos(2\phi)(4(\cos^2(2\phi) - 3)) \\
&= \sin^6 \theta(4(\cos^3(2\phi) - 3 \cos(2\phi))) \\
&= \sin^6 \theta \cos(6\phi)
\end{aligned}$$

$$\begin{aligned}
& (H_x \sin \theta \cos \phi + H_y \sin \theta \sin \phi + H_z \cos \theta)^2 \\
&= (H_x \sin \theta \cos \phi)^2 + (H_y \sin \theta \sin \phi)^2 + (H_z \cos \theta)^2 \\
&\quad + H_y H_z \sin(2\theta) \sin \phi + H_x H_z \sin(2\theta) \cos \phi + H_x H_y \sin^2 \theta \sin(2\phi)
\end{aligned}$$

We also define  $\overline{H}_{2\parallel} := H_{2\parallel} + \frac{H_{DMI}^2}{H_{ex}}$  which as  $H_{2\parallel}$  can be positive or negative while other internal fields are still all positive. After defining a new potential  $U$ , we get as final result

$$\begin{aligned}
U(\theta, \phi) := H_{ex} \frac{w_{ani}}{2M_s} &= \frac{1}{2} (H_{ex} \overline{H}_{2\parallel} + H_z^2) \cos^2 \theta - \frac{H_{ex} H_{\perp}}{6} \sin^6 \theta \cos(6\phi) \\
&\quad + \frac{\sin^2 \theta}{2} (H_y^2 \sin^2 \phi + H_x^2 \cos^2 \phi) + \frac{H_z}{2} \sin(2\theta) (H_y \sin \phi + H_x \cos \phi) \\
&\quad + \frac{H_x H_y}{2} \sin^2 \theta \sin(2\phi) - H_{DMI} \sin \theta (H_y \cos \phi - H_x \sin \phi) \\
&\quad - \frac{H^2 + H_{DMI}^2}{2}
\end{aligned} \tag{2.7}$$

The minima of  $U$  are equivalent to the minima of  $w_{ani}$ . To find minima of  $U$  we have to derive with respect to  $\theta$  and  $\phi$  and solve both

$$\frac{\partial U}{\partial \phi} = 0, \quad \frac{\partial U}{\partial \theta} = 0 \tag{2.8}$$

For the solutions of these equations we get stable states (minima) if

$$\begin{aligned}
& \frac{\partial^2 U}{\partial \phi^2}, \frac{\partial^2 U}{\partial \theta^2} > 0 \\
& \frac{\partial^2 U}{\partial \phi^2} \cdot \frac{\partial^2 U}{\partial \theta^2} - \left( \frac{\partial^2 U}{\partial \phi \partial \theta} \right)^2 > 0
\end{aligned} \tag{2.9}$$

With these conditions we can search minima of  $U$ , which is the task of the next section.

## 2.4. Field free case

First, we are interested in the anisotropy in the absence of an external magnetic field. Then the formula for  $U$  simplifies to

$$U(\theta, \phi) = \frac{1}{2} H_{ex} \bar{H}_{2\parallel} \cos^2 \theta - \frac{H_{ex} H_{\perp}}{6} \sin^6 \theta \cos(6\phi) - \frac{H_{DMI}^2}{2} \quad (2.10)$$

with the first derivatives

$$\begin{aligned} \frac{\partial U}{\partial \phi} &= H_{ex} H_{\perp} \sin^6 \theta \sin(6\phi) \\ \frac{\partial U}{\partial \theta} &= -\frac{1}{2} H_{ex} \bar{H}_{2\parallel} \sin(2\theta) - H_{ex} H_{\perp} \cos \theta \sin^5 \theta \cos(6\phi) \end{aligned}$$

Since the second derivatives are also needed later, they are listed here as well.

$$\begin{aligned} \frac{\partial^2 U}{\partial \phi^2} &= 6 H_{ex} H_{\perp} \sin^6 \theta \cos(6\phi) \\ \frac{\partial^2 U}{\partial \theta^2} &= -H_{ex} \bar{H}_{2\parallel} \cos(2\theta) - 5 H_{ex} H_{\perp} \cos^2 \theta \sin^4 \theta \cos(6\phi) + H_{ex} H_{\perp} \sin^6 \theta \cos(6\phi) \\ \frac{\partial^2 U}{\partial \phi \partial \theta} &= 6 H_{ex} H_{\perp} \cos \theta \sin^5 \theta \sin(6\phi) \end{aligned}$$

There are several solutions which zero the first derivatives. The first ones are  $\theta = \frac{\pi}{2}$  and  $\phi = n \cdot \frac{\pi}{6}$  for  $n = 0, 1, \dots, 11$ . Therefore,  $\vec{n}$  takes position in the xy-plane. For this solutions the second derivatives become

$$\frac{\partial^2 U}{\partial \phi^2} = \pm 6 H_{ex} H_{\perp}, \quad \frac{\partial^2 U}{\partial \theta^2} = H_{ex} \bar{H}_{2\parallel} \pm H_{ex} H_{\perp}, \quad \frac{\partial^2 U}{\partial \phi \partial \theta} = 0$$

The sign in front of  $H_{\perp}$  depends on what the integer  $n$  is. For odd  $n$  the sign is minus so the states are not stable any more since  $\frac{\partial^2 U}{\partial \phi^2} < 0$ . For an even  $n$ , due to the fact that we consider a positive  $H_{\perp}$ , the final stability condition is  $\bar{H}_{2\parallel} + H_{\perp} > 0$ . Since we assumed  $|\bar{H}_{2\parallel}| \gg H_{\perp}$  the result is that without an external magnetic field there are stable states for the Néel-vector in the xy-plane with  $\theta = \frac{\pi}{2}$  and  $\phi = n \cdot \frac{\pi}{3}$  for  $n = 0, 1, \dots, 5$  if  $\bar{H}_{2\parallel} > 0$  and unstable  $\bar{H}_{2\parallel} < 0$ .

The second solution for eq. 2.8 is  $\theta = 0$  and  $\phi \in [0, 2\pi)$ , which means that  $\vec{n}$  is aligned along the z-axis. The second derivatives in this case are

$$\frac{\partial^2 U}{\partial \phi^2} = 0, \quad \frac{\partial^2 U}{\partial \theta^2} = -H_{ex} \bar{H}_{2\parallel}, \quad \frac{\partial^2 U}{\partial \phi \partial \theta} = 0$$

For  $\overline{H}_{2\parallel} > 0$  this is an unstable state. For  $\theta = 0$  the function of  $U$  becomes a constant with respect to  $\phi$ . Therefore,  $U$  is minimal over the whole range of  $\phi$  for  $\overline{H}_{2\parallel} < 0$ . It would make sense in that case to consider  $U$  as a function that does only depend of  $\theta$  with a free parameter  $\phi$ . As it can be seen from the derivatives this gives a stable state if we minimize with respect to  $\theta$ , so this solution gives possible equilibrium states for the magnetic orientation.

There is also a third solution to get zero from the first derivatives, which is  $\phi = n \cdot \frac{\pi}{6}$  for  $n = 0, 1, \dots, 11$  and  $0 = -\overline{H}_{2\parallel} \pm H_{\perp} \sin^4 \theta$ . This can be solved for  $\theta$  only if  $|\frac{\overline{H}_{2\parallel}}{H_{\perp}}| \leq 1$ , which is a case that is not considered here. Therefore, this not a possible solution for the estimated values from the anisotropy fields.

We can extract from the obtained results that if  $\overline{H}_{2\parallel} < 0$ , the Néel vector will always align along the easy axis as long if there is no external magnetic field. If we otherwise consider  $\overline{H}_{2\parallel} > 0$  we will find that  $\vec{n}$  is stable in the easy plane in one of six degenerate solutions. Therefore we define the case  $\overline{H}_{2\parallel} < 0$  as easy axis phase and  $\overline{H}_{2\parallel} > 0$  as easy plane phase.

## 2.5. Uniaxial anisotropy

We will now add an external magnetic field into the calculations. The most complicated part in  $U$  is the one related to  $H_{\perp}$ . Therefore, we will first neglect  $H_{\perp}$  and later include it in the calculations.

### 2.5.1. Magnetic field parallel to the easy plane

First, we are interested in the stable states that occur if the magnetic field is applied perpendicular to the easy axis. As long as  $H_{\perp}$  is neglected, there is no asymmetry in the x- and y-axis, so we expect an equivalent behaviour for any direction of the magnetic field, as long as it is in the easy plane. Therefore we apply the magnetic field along the y-axis, giving the following formula for the potential.

$$U(\theta, \phi) = \frac{1}{2} H_{ex} \overline{H}_{2\parallel} \cos^2 \theta + \frac{H^2}{2} \sin^2 \theta \sin^2 \phi - H H_{DMI} \sin \theta \cos \phi - \frac{H^2 + H_{DMI}^2}{2} \quad (2.11)$$

We assume that the field is pointing in the positive y-direction, so  $H_y = H > 0$ . The first and second derivatives are

$$\begin{aligned}\frac{\partial U}{\partial \phi} &= \frac{H^2}{2} \sin^2 \theta \sin(2\phi) + HH_{DMI} \sin \theta \sin \phi \\ \frac{\partial U}{\partial \theta} &= -\frac{1}{2} H_{ex} \bar{H}_{2\parallel} \sin(2\theta) + \frac{H^2}{2} \sin(2\theta) \sin^2 \phi - HH_{DMI} \cos \theta \cos \phi\end{aligned}$$

$$\begin{aligned}\frac{\partial^2 U}{\partial \phi^2} &= H^2 \sin^2 \theta \cos(2\phi) + HH_{DMI} \sin \theta \cos \phi \\ \frac{\partial^2 U}{\partial \theta^2} &= -H_{ex} \bar{H}_{2\parallel} \cos(2\theta) + H^2 \cos(2\theta) \sin^2 \phi + HH_{DMI} \sin \theta \cos \phi \\ \frac{\partial^2 U}{\partial \phi \partial \theta} &= \frac{H^2}{2} \sin(2\theta) \sin(2\phi) + HH_{DMI} \cos \theta \sin \phi\end{aligned}$$

One solution for  $\theta$  and  $\phi$  to get zero from the first derivatives is  $\theta = 0$  and  $\phi = \frac{\pi}{2}, \frac{3\pi}{2}$  ( $\vec{n}$  on the z-axis). For this values the second derivatives give the result

$$\frac{\partial^2 U}{\partial \phi^2} = 0, \quad \frac{\partial^2 U}{\partial \theta^2} = -H_{ex} \bar{H}_{2\parallel} + H^2, \quad \frac{\partial^2 U}{\partial \phi \partial \theta} = \pm HH_{DMI}$$

This is an unstable state that has no longer to be investigated because

$$\frac{\partial^2 U}{\partial \phi^2} \cdot \frac{\partial^2 U}{\partial \theta^2} - \left( \frac{\partial^2 U}{\partial \phi \partial \theta} \right)^2 = -(HH_{DMI})^2 < 0.$$

Another solution for eq. 2.8 is  $\theta = \frac{\pi}{2}$  and  $\phi = 0, \pi$ , where  $\vec{n}$  is aligned along the x-axis. The second derivatives for this solution are

$$\frac{\partial^2 U}{\partial \phi^2} = H^2 \pm HH_{DMI}, \quad \frac{\partial^2 U}{\partial \theta^2} = H_{ex} \bar{H}_{2\parallel} \pm HH_{DMI}, \quad \frac{\partial^2 U}{\partial \phi \partial \theta} = 0$$

Therefore, this state has only two stability conditions, namely  $H^2 \pm HH_{DMI} > 0$  and  $H_{ex} \bar{H}_{2\parallel} \pm HH_{DMI} > 0$ . Under the constraint that we assumed  $H > 0$  the first condition is always fulfilled for  $\phi = 0$ . If we assume that the phase is easy axis, we see that  $\phi = \pi$  is not stable because  $H_{ex} \bar{H}_{2\parallel} - HH_{DMI} < 0$  for all  $H > 0$ . That means in the easy axis phase with  $\phi = 0$  the only remaining condition for stability is  $H > -\frac{H_{ex} \bar{H}_{2\parallel}}{H_{DMI}}$ .

For  $\phi = 0$  the second condition is also always fulfilled in the easy plane phase. Then the state is stable independent of  $H$ . Still in the easy plane phase but with  $\phi = \pi$  the effective condition for  $H$  to make a stable state is  $H > \max(\frac{H_{ex} \bar{H}_{2\parallel}}{H_{DMI}}, H_{DMI})$ , while it depends on the temperature which value is larger.

Also a third solution can be found, which is  $\phi = 0, \pi$  and  $\sin \theta = \mp \frac{HH_{DMI}}{H_{ex}\bar{H}_{2\parallel}}$ . The sign of the sin depends on  $\phi$ . Since  $\theta \in [0, \pi]$  where the sin is positive, the solution for  $\phi = 0$  with  $\sin \theta = -\frac{HH_{DMI}}{H_{ex}\bar{H}_{2\parallel}}$  is only possible in the easy axis phase, while the other one only occurs in the easy plane phase. For these cases the second derivatives take the values

$$\begin{aligned}\frac{\partial^2 U}{\partial \phi^2} &= H^2 \sin^2 \theta \pm HH_{DMI} \sin \theta = \left( \frac{HH_{DMI}}{H_{ex}\bar{H}_{2\parallel}} \right)^2 (H^2 \mp H_{ex}\bar{H}_{2\parallel}) \\ \frac{\partial^2 U}{\partial \theta^2} &= -H_{ex}\bar{H}_{2\parallel} \cos 2\theta \pm HH_{DMI} \sin \theta = -H_{ex}\bar{H}_{2\parallel} \cos^2 \theta + H_{ex}\bar{H}_{2\parallel} \sin^2 \theta \pm HH_{DMI} \sin \theta \\ &= -H_{ex}\bar{H}_{2\parallel} \cos^2 \theta \\ \frac{\partial^2 U}{\partial \phi \partial \theta} &= 0\end{aligned}$$

In the easy plane phase this can not be a stable state. In the easy axis phase there is  $\frac{\partial^2 U}{\partial \phi^2}, \frac{\partial^2 U}{\partial \theta^2} > 0$ . That means for  $\phi = 0$  and  $\sin \theta = -\frac{HH_{DMI}}{H_{ex}\bar{H}_{2\parallel}}$  there is a stable state, where  $\vec{n}$  is positioned perpendicular to the y-axis. We see here that for  $H = 0$  we get  $\theta = 0$  so  $\vec{n}$  is on the z-axis and rotates out of it with rising field up to  $H = -\frac{H_{ex}\bar{H}_{2\parallel}}{H_{DMI}}$ . For higher fields  $\sin \theta$  would have to be greater than 1 which is not possible. After reaching that point of magnetic field the previous discussed case  $\theta = \frac{\pi}{2}$  and  $\phi = 0$  applies.

We can see from the results that in the easy axis phase  $\vec{n}$  is on the easy axis for  $H = 0$  and rotates out of the z-axis within the xz-plane until  $H = -\frac{H_{ex}\bar{H}_{2\parallel}}{H_{DMI}}$  where it then is on the x-axis and invariant for stronger fields.

In the easy plane phase  $\vec{n}$  is stable on the x-axis for every external field strength.

### 2.5.2. Magnetic field parallel to the easy axis

After we know the stable states for  $\vec{n}$  if the magnetic field lies in the easy plane, we want it now to be aligned along the easy axis. Again we assume that the field is aligned in the positive direction of the z-axis ( $H_z = H > 0$ ). The potential then becomes

$$U(\theta, \phi) = U(\theta) = \frac{1}{2} (H_{ex}\bar{H}_{2\parallel} + H^2) \cos^2 \theta - \frac{H^2 + H_{DMI}^2}{2}, \quad (2.12)$$

$$(2.13)$$

which only depends on  $\theta$ . Therefore, it will only be minimized with respect to  $\theta$ . Its derivative is

$$\frac{\partial U}{\partial \theta} = -\frac{1}{2} (H_{ex} \bar{H}_{2\parallel} + H^2) \sin(2\theta)$$

The solutions for  $\frac{\partial U}{\partial \theta} = 0$  are  $\theta = 0$  ( $\vec{n}$  on z-axis) and  $\theta = \frac{\pi}{2}$  ( $\vec{n}$  in xy-plane). The second derivative of  $U(\theta)$  is

$$\frac{\partial^2 U}{\partial \theta^2} = - (H_{ex} \bar{H}_{2\parallel} + H^2) \cos(2\theta)$$

so we can see, that for  $\theta = 0$  the state is stable in the easy axis phase if  $H^2 < -H_{ex} \bar{H}_{2\parallel}$  but unstable in the easy plane phase. Looking at  $\theta = \frac{\pi}{2}$  and considering the easy axis phase we observe that the phase is stable for  $H^2 > -H_{ex} \bar{H}_{2\parallel}$ . If we instead consider the easy plane phase the state is stable for every value of  $H$ . So we can see that in the easy plane phase where  $\bar{H}_{2\parallel} > 0$  we have a stable state in an arbitrary direction in the easy plane for  $\vec{n}$  independent of the field strength, while in the easy axis phase with  $\bar{H}_{2\parallel} < 0$   $\vec{n}$  for low fields is placed on the easy axis and flips into the easy plane instantly at  $H = \sqrt{-H_{ex} \bar{H}_{2\parallel}}$ .

### 2.5.3. Arbitrary magnetic field

Lastly, in the approximation, that  $H_{\perp}$  can be neglected we are interested in the stable states if the field is arbitrary. x- and y-axis are still equivalent and therefore we consider the field only to have x- and z-components ( $H_y = 0$ ). The potential then is

$$U(\theta, \phi) = \frac{1}{2} (H_{ex} \bar{H}_{2\parallel} + H_z^2) \cos^2 \theta + \frac{H_x^2}{2} \sin^2 \theta \cos^2 \phi + \frac{H_x H_z}{2} \sin(2\theta) \cos \phi - H_x H_{DMI} \sin \theta \sin \phi - \frac{H^2 + H_{DMI}^2}{2}. \quad (2.14)$$

It has the derivatives

$$\begin{aligned} \frac{\partial U}{\partial \phi} &= -\frac{H_x H_z}{2} \sin(2\theta) \sin \phi - \frac{H_x^2}{2} \sin^2 \theta \sin(2\phi) + H_x H_{DMI} \sin \theta \cos \phi \\ \frac{\partial U}{\partial \theta} &= -\frac{1}{2} (H_{ex} \bar{H}_{2\parallel} + H_z^2) \sin(2\theta) + \frac{H_x^2}{2} \sin(2\theta) \cos^2 \phi \\ &\quad + H_x H_z \cos(2\theta) \cos \phi + H_x H_{DMI} \cos \theta \sin \phi \end{aligned}$$

---

2. Analysis of the anisotropy in hematite

---

$$\begin{aligned}\frac{\partial^2 U}{\partial \phi^2} &= -\frac{H_x H_z}{2} \sin(2\theta) \cos \phi - H_x^2 \sin^2 \theta \cos(2\phi) - H_x H_{DMI} \sin \theta \sin \phi \\ \frac{\partial^2 U}{\partial \theta^2} &= -\left(H_{ex} \bar{H}_{2\parallel} + H_z^2\right) \cos(2\theta) + H_x^2 \cos(2\theta) \cos^2 \phi \\ &\quad - 2H_x H_z \sin(2\theta) \cos \phi - H_x H_{DMI} \sin \theta \sin \phi \\ \frac{\partial^2 U}{\partial \phi \partial \theta} &= -H_x H_z \cos(2\theta) \sin \phi - \frac{H_x^2}{2} \sin(2\theta) \sin(2\phi) + H_x H_{DMI} \cos \theta \cos \phi\end{aligned}$$

The first solution to get zero from the first derivatives is  $\theta = 0$  and  $H_z \cos \phi + H_{DMI} \sin \phi = 0$  or  $\tan \phi = -H_z/H_{DMI}$ . In this state it is  $\frac{\partial^2 U}{\partial \phi^2} = 0$  for  $\theta = 0$  and

$$\frac{\partial^2 U}{\partial \phi \partial \theta} = -H_x H_z \sin \phi + H_x H_{DMI} \cos \phi$$

which is zero if  $H_x = 0$  or  $H_{DMI}/H_z = \tan \phi$ .  $H_x = 0$  is a case that has already been discussed and therefore we want to consider  $H_x \neq 0$ . The second possibility for this expression to be zero would lead to  $H_{DMI}/H_z = -H_z/H_{DMI}$  which is obviously not possible. Therefore the expression does not equal zero and the state is unstable because

$$\frac{\partial^2 U}{\partial \phi^2} \cdot \frac{\partial^2 U}{\partial \theta^2} - \left(\frac{\partial^2 U}{\partial \phi \partial \theta}\right)^2 = -(-H_x H_z \sin \phi + H_x H_{DMI} \cos \phi)^2 < 0.$$

Another solution is  $\theta = \frac{\pi}{2}$  and  $\phi = \frac{\pi}{2}, \frac{3\pi}{2}$ . For this solution the second derivatives take the values

$$\begin{aligned}\frac{\partial^2 U}{\partial \phi^2} &= H_x^2 \mp H_x H_{DMI} \\ \frac{\partial^2 U}{\partial \theta^2} &= H_{ex} \bar{H}_{2\parallel} + H_z^2 \mp H_x H_{DMI} \\ \frac{\partial^2 U}{\partial \phi \partial \theta} &= \pm H_x H_z\end{aligned}$$

where the sign depends on the value for  $\phi$ . From this we can select the following stability conditions.

$$\begin{aligned}H_x^2 \mp H_x H_{DMI} &> 0 \\ H_{ex} \bar{H}_{2\parallel} + H_z^2 \mp H_x H_{DMI} &> 0 \\ H_x [H_{ex} \bar{H}_{2\parallel} H_x \mp H_{DMI} (H_x^2 + H_z^2) \mp H_{ex} \bar{H}_{2\parallel} H_{DMI} + H_{DMI}^2 H_x] &> 0\end{aligned}$$

Effectively this gives one condition  $|H_x| > H_{DMI}$  and another condition covered by the last condition written above because if only one of the first conditions would hold, the last one can not be fulfilled. We will first calculate the critical field from the third condition (where the condition does not hold any more) to see which of the both conditions is stronger. To find this field, we define  $H_x = H \sin \psi$  and  $H_z = H \cos \psi$  with  $H > 0$ . Then we get the relation at the critical point

$$\begin{aligned}
 0 &= [H_{ex}\bar{H}_{2\parallel}H \sin \psi \mp H_{DMI}H^2 \mp H_{ex}\bar{H}_{2\parallel}H_{DMI} + H_{DMI}^2H \sin \psi] \\
 \Rightarrow 0 &= H^3(\mp H_{DMI} \sin \psi) + H^2(H_{ex}\bar{H}_{2\parallel} \sin^2 \psi + H_{DMI}^2 \sin^2 \psi) + H(\mp H_{ex}\bar{H}_{2\parallel}H_{DMI} \sin \psi) \\
 \Rightarrow 0 &= H^2 \mp H \left( \frac{H_{ex}\bar{H}_{2\parallel} + H_{DMI}^2}{H_{DMI}} \sin \psi \right) + H_{ex}\bar{H}_{2\parallel} \\
 \Rightarrow H &= \pm \left( \frac{H_{ex}\bar{H}_{2\parallel} + H_{DMI}^2}{2H_{DMI}} \sin \psi \right) \pm \sqrt{\left( \frac{H_{ex}\bar{H}_{2\parallel} + H_{DMI}^2}{2H_{DMI}} \right)^2 \sin^2 \psi - H_{ex}\bar{H}_{2\parallel}}
 \end{aligned}$$

We only take the solutions in which  $H$  is positive. There we see since  $H_x = H \sin \psi$  that the critical  $H_x$  from this condition is greater than  $H_{DMI}$  showing that this is the stronger condition and the calculated critical point defines a phase transition.

For the easy plane phase this result is not real for all  $\psi$ , so there is no phase transition, implying that the state is either stable or unstable for all values of  $H$  and  $\psi$ . Since there are stable states in the easy plane phase equivalent to this from the first two considered cases, we can conclude that this state is always stable in the easy plane phase.

In the easy axis phase we see that the transition point depends on the direction of the field, i.e. for  $\vec{H} \parallel \hat{z}$  we observe the same result as before and for  $\vec{H} \parallel \hat{x}$  the transition is at  $H = -\frac{H_{ex}\bar{H}_{2\parallel}}{H_{DMI}}$  as also previously obtained for  $\vec{H} \parallel \hat{y}$ . Here we also see that for  $\psi = \frac{\pi}{2}$  where  $\vec{n}$  is aligned in positive direction of the x-axis only the  $\phi = \frac{\pi}{2}$  solution gives a positive  $H$  and similar with  $\psi = \frac{3\pi}{2}$  and  $\phi = \frac{3\pi}{2}$ . This shows that  $\vec{n}$  does not only orientate itself orthogonal to  $\vec{H}$  but also it has a preferred direction in the easy plane depending on the orientation of  $\vec{H}$  ( $90^\circ$  in clockwise direction to  $\vec{H}$ ), which results from the  $DMI$ -field.

From the stability conditions we can see that the obtained state is stable if the field is larger than the phase transition field in the easy axis phase. If  $H$  is lower we can assume from the previous results, that  $\vec{n}$  rotates from the z-axis into the obtained solution with rising field strength or flips instantly (for  $\vec{H} \parallel \hat{z}$ ).

### 2.5.4. Brief summary of the results

Up to this point we obtained that every time  $\vec{n}$  tries to be orthogonal to  $\vec{H}$  which makes sense since  $\vec{n}$  is always orthogonal to the magnetization inside the crystal, which couples to  $\vec{H}$ . In the easy axis phase we see that for low magnetic fields  $\vec{n}$  is aligned on or close to the z-axis because of the uniaxial anisotropy field. If the field rises and

is not parallel to the z-axis,  $\vec{n}$  rotates out of the axis into the easy plane where it has a favoured direction in relation to  $\vec{H}$  due to the *DMI*-field. If the field is aligned on the z-axis there is no rotation but a instant flip of  $\vec{n}$  from the easy axis in the easy plane in an arbitrary direction. After  $\vec{n}$  has reached the state in the xy-plane it is invariant if the field increases. However, the magnetization has to increase with the field meaning that the sublattices do not have antiparallel magnetizations any more. This is a known phenomenon and this state is called spin flop phase [18]. In the easy plane phase we can always find a stable state whose stability is independent of the strength of the field. All this holds without considering  $H_{\perp}$  and the behaviour of  $\vec{n}$  may change if we take  $H_{\perp}$  into account.

## 2.6. General anisotropy

We will now add  $H_{\perp}$  into the calculations. We do not expect much to change from the previous results in the approximation that  $H_{\perp}$  is small. Since we already found solutions for the case without  $H_{\perp}$ , we will not search for new ones but try if the old solution still hold to compare the results. The solutions now have to fulfil the additional conditions

$$\begin{aligned} 0 &= H_{\perp} \sin^6 \theta \sin(6\phi) \\ 0 &= H_{\perp} \cos \theta \sin^5 \theta \cos(6\phi). \end{aligned}$$

This are the derivatives of the  $H_{\perp}$  part in  $U$  with respect to  $\phi$  and  $\theta$ . Let  $U_0$  be the potential without  $H_{\perp}$ . Then the second derivatives are

$$\begin{aligned} \frac{\partial^2 U}{\partial \phi^2} &= \frac{\partial^2 U_0}{\partial \phi^2} + 6H_{ex}H_{\perp} \sin^6 \theta \cos(6\phi) \\ \frac{\partial^2 U}{\partial \theta^2} &= \frac{\partial^2 U_0}{\partial \theta^2} - 5H_{ex}H_{\perp} \cos^2 \theta \sin^4 \theta \cos(6\phi) + H_{ex}H_{\perp} \sin^6 \theta \cos(6\phi) \\ \frac{\partial^2 U}{\partial \phi \partial \theta} &= \frac{\partial^2 U_0}{\partial \phi \partial \theta} + 6H_{ex}H_{\perp} \cos \theta \sin^5 \theta \sin(6\phi). \end{aligned}$$

We can directly observe that for states with  $\theta = 0$  nothing changes, since in every term a  $\sin \theta$  occurs, which is 0 in that case. Therefore, the states with  $\theta = 0$  will not be investigated again in this section.

### 2.6.1. Magnetic field parallel to the easy plane

As in sec. 2.5 we will consider  $\vec{H} \parallel \hat{y}$  here (again with  $H_y = H > 0$ ). In the previous section we obtained that  $\vec{n}$  is invariant in the easy plane phase and rotates from the easy axis into the easy plane until  $H = -\frac{H_{ex}\vec{H}_{2\parallel}}{H_{DMI}}$  where  $\vec{n}$  is then placed in the easy plane and perpendicular to  $\vec{H}$ .

In this case the only remaining solution (besides  $\theta = 0$ ) is  $\theta = \frac{\pi}{2}$  and  $\phi = 0, \pi$ . For this values the second derivatives are

$$\begin{aligned}\frac{\partial^2 U}{\partial \phi^2} &= H^2 \pm HH_{DMI} + 6H_{ex}H_{\perp} \\ \frac{\partial^2 U}{\partial \theta^2} &= H_{ex}\bar{H}_{2\parallel} \pm HH_{DMI} + H_{ex}H_{\perp} \\ \frac{\partial^2 U}{\partial \phi \partial \theta} &= 0\end{aligned}$$

Therefore the state is stable if the two conditions hold.

$$\begin{aligned}H^2 \pm HH_{DMI} + 6H_{ex}H_{\perp} &> 0 \\ H_{ex}\bar{H}_{2\parallel} \pm HH_{DMI} + H_{ex}H_{\perp} &> 0\end{aligned}$$

Here, it is reasonable to separate the cases. For  $\phi = 0$  the first condition is always fulfilled and in the easy plane phase the second as well. In the easy axis phase the state is stable as long as  $H > -\frac{H_{ex}}{H_{DMI}}(\bar{H}_{2\parallel} + H_{\perp})$ .

If we now consider  $\phi = \pi$  we can observe that the state cannot be stable in the easy axis phase because we assumed  $H > 0$  and  $\bar{H}_{2\parallel} + H_{\perp} < 0$ .

In the easy plane phase we get a stable case for

$$H > \max \left( \frac{H_{DMI}}{2} + \sqrt{\left(\frac{H_{DMI}}{2}\right)^2 - 6H_{ex}H_{\perp}}, \frac{H_{ex}}{H_{DMI}}(\bar{H}_{2\parallel} + H_{\perp}) \right)$$

which is similar to the case without  $H_{\perp}$  with only slightly different formulas for the stability that now have a contribution of  $H_{\perp}$ .

Even though the state where  $\vec{n}$  rotated out of the z-axis with a harmonic function is not stable any more, it would be reasonable if there is still a state that describes how  $\vec{n}$  rotates away from a state close to the z-axis since the uniaxial anisotropy is still much larger than the in plane anisotropy. It may be just be a state difficult to find analytically.

### 2.6.2. Magnetic field parallel to the easy axis

In sec. 2.5 we found that in the easy axis phase  $\vec{n}$  is aligned on the easy axis until the external field reaches  $\sqrt{-H_{ex}\bar{H}_{2\parallel}}$  and then flips into an arbitrary direction in the easy plane. In the easy plane phase  $\vec{n}$  was invariant by changing the field and place din the easy plane. If  $H_{\perp}$  is included  $U$  is not a function of  $\theta$  alone any more. Still the  $\theta = 0$  solution will not change but for  $\theta = \frac{\pi}{2}$  the dependency on  $\phi$  changes in the

way that  $\theta = \frac{\pi}{2}$  only can be an extremum if  $\phi = n \cdot \frac{\pi}{6}$  for  $n = 0, 1, \dots, 11$ . The second derivatives of the potential are

$$\begin{aligned}\frac{\partial^2 U}{\partial \phi^2} &= \pm 6H_{ex}H_{\perp} \\ \frac{\partial^2 U}{\partial \theta^2} &= H_{ex}\overline{H}_{2\parallel} + H_z^2 \pm H_{ex}H_{\perp} \\ \frac{\partial^2 U}{\partial \phi \partial \theta} &= 0.\end{aligned}$$

From the first equation we directly get that only for  $\phi = n \cdot \frac{\pi}{3}$  with  $n = 0, 1, \dots, 5$  can give a stable state. The remaining stability condition requires

$$H_z^2 > -H_{ex}(\overline{H}_{2\parallel} + H_{\perp})$$

In the easy plane phase this is a trivial statement that always holds but in the easy axis phase there is a phase transition of the state at  $H_z = \sqrt{-H_{ex}(\overline{H}_{2\parallel} + H_{\perp})}$ . We see that the result is almost the same as without  $H_{\perp}$  with one change that  $\vec{n}$  does not flip instantly because between the solutions  $\theta = 0$  and  $\theta = \frac{\pi}{2}$  since they have different transition points now. In between it would make sense if  $\vec{n}$  rotates into the easy plane but since  $|\overline{H}_{2\parallel}| \gg H_{\perp}$  the transition should still be very narrow. A second difference occurring from  $H_{\perp}$  is that it is not completely any more where on the easy plane  $\vec{n}$  goes but it has six stable orientations.

### 2.6.3. Arbitrary magnetic field

Since in the previous section we chose the field to be in the xz-plane, it will not be completely arbitrary now but again be in the xz-plane. In this case remains and is  $\theta = \frac{\pi}{2}$  and  $\phi = \frac{\pi}{2}, \frac{3\pi}{2}$ . The second derivatives for this solution have the following form now.

$$\begin{aligned}\frac{\partial^2 U}{\partial \phi^2} &= H_x^2 \mp H_x H_{DMI} - 6H_{ex}H_{\perp} \\ \frac{\partial^2 U}{\partial \theta^2} &= H_{ex}\overline{H}_{2\parallel} + H_z^2 \mp H_x H_{DMI} - H_{ex}H_{\perp} \\ \frac{\partial^2 U}{\partial \phi \partial \theta} &= \pm H_x H_z\end{aligned}$$

Besides the conditions  $\frac{\partial^2 U}{\partial \theta^2}, \frac{\partial^2 U}{\partial \phi^2} > 0$  the state must also fulfil

$$(H_x^2 \mp H_x H_{DMI} - 6H_{ex}H_{\perp}) (H_{ex}\overline{H}_{2\parallel} + H_z^2 \mp H_x H_{DMI} - H_{ex}H_{\perp}) - (H_x H_z)^2 > 0$$

---

## 2. Analysis of the anisotropy in hematite

---

to be stable. This is a system of equations depending on two variables up to third order, which makes it difficult to be analyzed. Also as obtained previously we cannot find the stable states for some magnetic fields in an analytical way. Therefore, a numerical approach is more reasonable from now to on the one hand find the behaviour of  $\vec{n}$  in this model and on the other hand to compare it to the solutions of the simplified case in sec. 2.5.

## 3. Numerical investigation of the anisotropy in easy axis phase

### 3.1. Analysing method

To find minima of the anisotropy energy we consider the equations of motion for the angles  $\theta$  and  $\phi$

$$\ddot{\theta} + \gamma \dot{\theta} + \frac{\partial U}{\partial \theta} = 0 \quad (3.1)$$

$$\ddot{\phi} + \gamma \dot{\phi} + \frac{\partial U}{\partial \phi} = 0 \quad (3.2)$$

with  $\gamma > 0$ . The time evolution of the solutions to this equations will result in a minimum of  $U$ . This happens because the system will relax to certain values of  $\theta$  and  $\phi$  due to the damping  $\gamma$  and if then both derivatives are zero in the relaxed state we have  $\frac{\partial U}{\partial \theta}, \frac{\partial U}{\partial \phi} = 0$ . Around a maximum small deviations produce new dynamics in a system i.e. deviations of the maximum cause the derivatives to grow again, so the system can not relax into a maximum. Effectively the angles oscillate into a minimum by time.

In eq. 3.1 and 3.2 a constant in front of the derivatives of  $U$  was omitted. This constant only fixes the units of the equations and does not change the results. Also the constant  $\gamma$  will be taken to be dimensionless which then gives the time dimension 1 as well.

We will first consider the easy axis phase. In the computations the form of  $U$  in eq. 2.7 was used. The values for the fields were chosen to be  $H_{ex} = 1040$  T,  $\overline{H}_{2\parallel} = 24.09$  mT,  $H_{\perp} = 961$   $\mu$ T,  $H_{DMI} = 2.75$  T and the damping constant was set to  $\gamma = 3$ . These values were based on the ones estimated in [13–16] but also the freedom that this is a work not based on real values was used to change the values if different values show the behaviour of  $\vec{n}$  in a more clear way. For example,  $H_{\perp}$  was chosen very high considering that we assumed in the beginning  $|\overline{H}_{2\parallel}| \gg H_{\perp}$ , to eventually see an influence of this in-plane anisotropy on the Néel vector. This has to be respected if one wants to compare this results to experimentally obtained values. For given  $\vec{H}$  the differential equations were numerically solved with Wolfram Mathematica from the time  $t = 0$  to  $t = 20$ . To get the values for the minimum the solutions for  $\theta$  and  $\phi$  were averaged in the range from  $t = 5$  to  $t = 20$  when the oscillation has dropped. This method is visualised in Fig. 3.1 with the exemplary values of  $H_x = H_y = 0$  T and  $H_z = 6$  T.

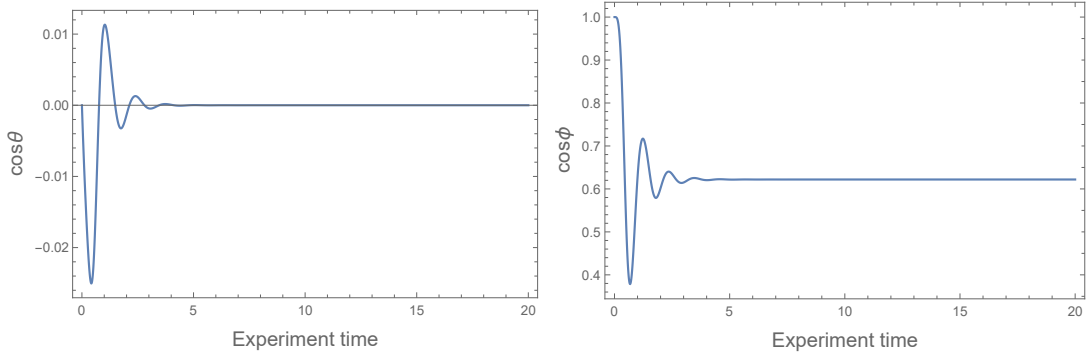


Figure 3.1.: Cosine of the solution to eq. 3.1 and 3.2 is plotted against time. The magnetic field was placed on the z-axis with a strength of 6 T and the initial conditions were  $\theta(0) = \frac{\pi}{2}$ ,  $\phi(0) = 0$ ,  $\dot{\theta}(0) = 0.1$ ,  $\dot{\phi}(0) = 0.1$ . After  $t = 5$  the oscillation is almost zero, so to get the equilibrium value we average from that point to  $t = 20$  giving  $\cos \theta = 0$  and  $\cos \phi = 0.667$ .

With this method we will scan through different values for the magnetic field and the direction of it to observe the behaviour of the stable states. In an experiment we can not measure  $\vec{n}$  directly but there are quantities that directly depend on  $\vec{n}$ . Therefore we introduce the spin hall magnetoresistance [19, 20] which can be measured, here defined over

$$R_{xx} = 1 - n_y^2, R_{yy} = 1 - n_x^2 \quad (3.3)$$

From this we can make statements about the orientation of the Néel vector and there can be qualitative comparisons to experimental data. There is also a non diagonal term  $R_{xy} = n_x n_y$  but this does not give us new information about how  $\vec{n}$  behaves, so we will neglect it.

### 3.2. One dimensional scans

First, to get in touch with the analysing method we do some one dimensional scans of the system, i.e. magnetic field strength or direction of the field (characterized by an angle) will be fixed while the other scans through different values. For every scan we start with the initial conditions  $\theta(0) = 0$ ,  $\phi(0) = 0$  which is a stable state in the absence of a magnetic field and  $\dot{\theta}(0) = 0.1$ ,  $\dot{\phi}(0) = 0.1$  to give the system some dynamics. The initial conditions for  $\theta$  and  $\phi$  then change after every point in the scan to the latest obtained result to ensure that the angles are still close to the minimum, while the initial conditions of the derivatives stay the same through the whole scan. The scans were done in 100 steps on the magnetic field strength from 0 T up to 13.5 T and the angle for direction of the field was scanned in 100 steps from 0 to  $2\pi$ . The data points were also joined after every scan so we can see changes of the system in a better

way. In the following we will take a look at the previously defined magnetoresistances and the "raw" data from the scans is presented in the appendix.

### 3.2.1. Scan with fixed field orientation

Beginning with fixed orientations for the field we can observe in Fig. 3.2 that for each of the chosen directions the magnetoresistance (and therefore the Néel vector) becomes constant after a certain field. If we look at the case  $\vec{H} \parallel \hat{z}$ , one can observe how the magnetic field overcomes the force that holds  $\vec{n}$  on the easy axis at  $H \approx 5$  T, which is the value of  $\sqrt{H_{ex}(-\bar{H}_{2\parallel} + H_{\perp})}$  and almost instantly flips  $\vec{n}$ . This is the result that was predicted in Sec. 2.6 by the analytical solutions.

For the other two orientations we can see that the Néel vector moves only perpendicular to the chosen orientation. Therefore, the magnetization is always aligned parallel to the magnetic field and we would expect  $\vec{n}$  to place itself in the easy plane if  $H$  increases. This can also be observed by the decreasing magnetoresistance, e.g.  $R_{xx}$  decreases for  $H \parallel \hat{x}$  with rising field. In contrast to the situation with the field on the easy axis the Néel vector rotates in its saturation state with intermediate steps between  $\vec{n} \parallel \hat{z}$  and  $\vec{n} \parallel \hat{x}, \hat{y}$ . The saturation in this case is reached at around 9 T, with some differences in  $H \parallel \hat{x}$  and  $H \parallel \hat{y}$  maybe due to the influence of  $H_{\perp}$ . From the analytical solution in sec 2.5 we would expect the critical field to be  $H = -\frac{H_{ex}\bar{H}_{2\parallel}}{H_{DMI}} = 9.09$  T, which fits well on the data. Even though we could not find the relation that describes the rotation into the saturation after including  $H_{\perp}$  we still assumed it to happen after the results without  $H_{\perp}$  and the assumption that  $H_{\perp}$  is small compared to the other fields.

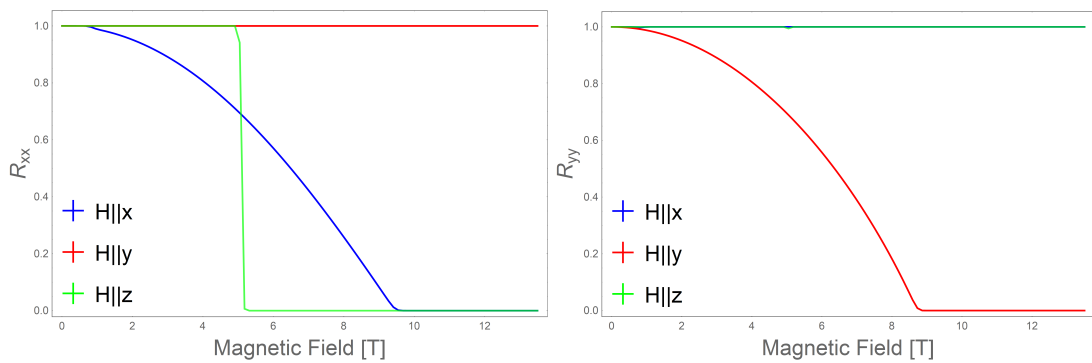


Figure 3.2.: Spin Hall magnetoresistance for the magnetic field aligned in a fixed direction in the easy axis phase.

From this we can extract three states of the magnetic field. For  $H < 5$  T the strongest effect on the Néel vector is the uniaxial isotropy field, i.e.  $\vec{n}$  tries to stay along the

easy axis. If  $\vec{H}$  is parallel to the z-axis in this state  $\vec{n}$  is invariant and if not the rotation away from the z-axis is still small. Between the saturation of the  $\vec{H} \parallel \hat{z}$  and the  $\vec{H} \parallel \hat{x}, \hat{y}$  case is the next state because depending on the field orientation  $\vec{n}$  is still moving or already saturated. The final interesting state is if all solutions are saturated which happens after about  $H = 9.5$  T.

### 3.2.2. Scan with fixed field strength

The scans with fixed fields were separated into three different planes, where the magnetic field rotates. We have a scan through the xy-plane ( $\alpha$ ) and the xz-plane ( $\beta$ ). If there would only be an uniaxial anisotropy, this would have been enough to cover up all different states but due to the in-plane anisotropy x-axis and y-axis are not equivalent. Therefore, also a scan through the yz-plane ( $\delta$ ) was done. The scans will from now on be named by the letters in the brackets and the magnetic fields depending on the scan are listed in Tab. 3.1.

| Scan     | $H_x$           | $H_y$           | $H_z$           |
|----------|-----------------|-----------------|-----------------|
| $\alpha$ | $H \cos \alpha$ | $H \sin \alpha$ | 0               |
| $\beta$  | $H \sin \beta$  | 0               | $H \cos \beta$  |
| $\delta$ | 0               | $H \sin \delta$ | $H \cos \delta$ |

Table 3.1.: Magnetic fields for the different scans.  $H$  is set constant and the angle scans from 0 to  $2\pi$ .

The values for the magnetic field strength were chosen to be 4,7 and 10 T so each of the above discussed states is covered. The result of the scans are visualized in Fig. 3.3, 3.4 and 3.5.

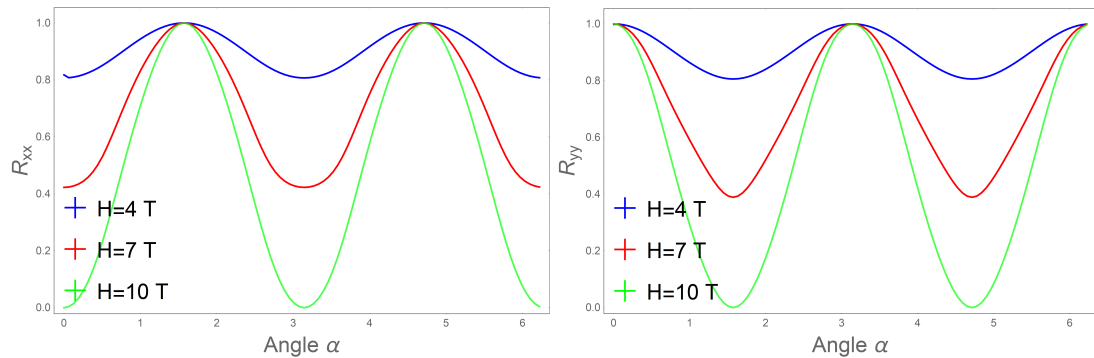


Figure 3.3.: Spin Hall magnetoresistance for the magnetic field rotation in the xy-plane with fixed field strength in the easy axis phase.

In the  $\alpha$ -scan we can observe that the easy plane part of  $\vec{n}$  rotates away from the magnetic field. This scan demonstrated very well how the external field overcomes

### 3. Numerical investigation of the anisotropy in easy axis phase

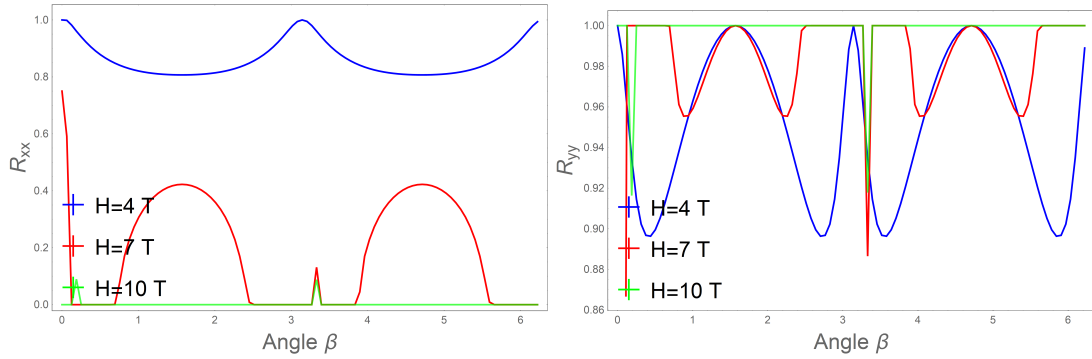


Figure 3.4.: Spin Hall magnetoresistance for the magnetic field rotation in the  $xz$ -plane with fixed field strength in the easy axis phase.

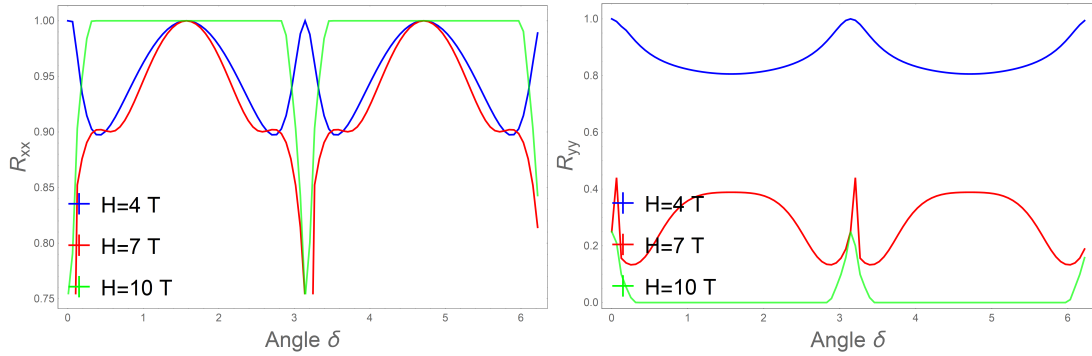


Figure 3.5.: Spin Hall magnetoresistance for the magnetic field rotation in the  $yz$ -plane with fixed field strength in the easy axis phase.

internal effects since for  $H = 4$  T both magnetoresistances are close to 1 so  $\vec{n}$  rotates close to the easy axis and they decrease for higher fields that for  $H = 10$  T  $\vec{n}$  moves only in the easy axis. From the scans with fixed orientation and the orthogonality of  $\vec{n}$  and  $\vec{m}$  this behaviour was the expected one.

We can see that in the  $\beta$ -scan  $n_x$  is almost 0 every time and has only a small oscillation away from 0 for small fields and if the field is not aligned on the  $x$ -axis. For high field  $\vec{n}$  points in  $y$  direction, while for small fields it has a  $z$  contribution if  $H \neq H_z$  where  $\vec{n}$  is on the easy axis. In between of these phenomenons  $\vec{n}$  gets a bigger  $y$  component and only rotates out of the  $y$ -axis if  $\vec{H}$  is far away from the easy axis. This again was expected to happen since we know how  $\vec{n}$  behaves for different fields on the  $x$ - and  $z$ -axis.

For the case where  $\vec{H} \parallel \hat{z}$  we get an unexpected result since we would expect no change in the  $R_{ii}$  at this point. It would not make sense to have such a behaviour of the system. The reason for that we observe this is the distance between the steps in the measurement. The number of steps was limited due to the technical resources

but for a higher number of steps in this region we should not observe this singularity. Therefore, we will consider the part of the scan where  $\beta = \pi$  as unphysical and exclude it of the discussion.

The  $\delta$ -scan gives results almost similar to the  $\beta$ -scan and again we have the unexpected singularity at  $\delta = \pi$ . Besides, this result is as expected but does not demonstrate the in-plane anisotropy since x- and y-axis did behave similar.

### 3.3. Two dimensional scan

After the scans with one fixed parameter, again a scan was made but now with both parameters moving to see the qualitative dependence of the magnetic field onto the stable states in  $U$ . This time the scans were done in 200 steps for the field strength and direction each. The results of these scans are plotted in Fig. 3.6, 3.7 and 3.8.

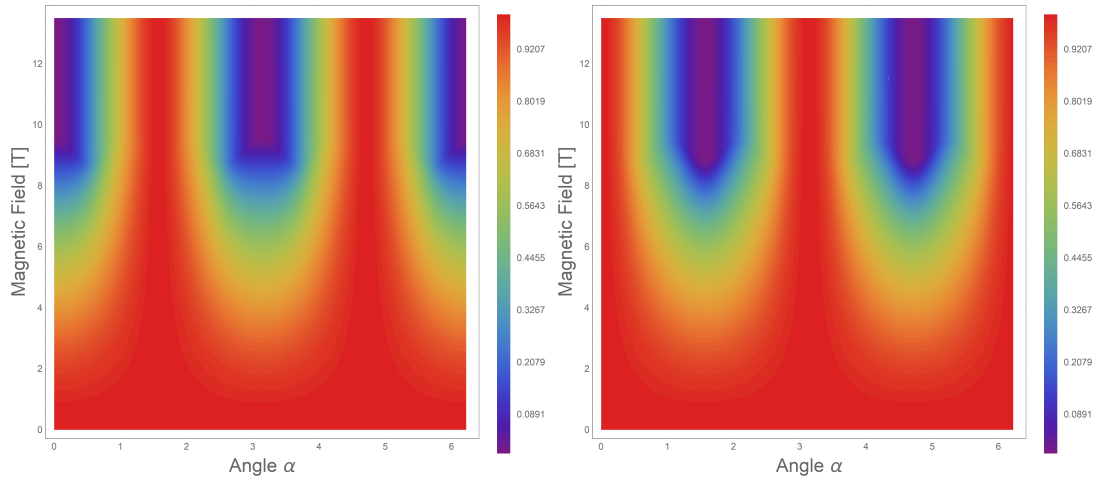


Figure 3.6.: Spin Hall magnetoresistance for different magnetic field strengths and directions in the xy-plane in the easy axis phase. The colourmap indicates the value for  $R_{xx}$  on the left and  $R_{yy}$  on the right.

We can see that for significantly low magnetic fields in every direction the Néel vector is aligned on the z-axis since the magnetoresistances are zero. In the  $\alpha$ -scan again the expected behaviour can be observed that  $\vec{n}$  rotates away from the field and that for high fields  $\vec{n}$  lies in the xy-plane.

In the  $\beta$ - and  $\delta$ -scan we see again that the process to saturation for rising fields happens in a small range if the field is close to the z-axis. When the field rotates away from the z-axis the rotation of  $\vec{n}$  goes over a longer range until the saturation is reached. For the field directly on the z-axis we can make no comment on the behaviour since we have again the singularity that occurred from the small number of steps in the scan but we know how  $\vec{n}$  behaves at this point from the one dimensional scans.

### 3. Numerical investigation of the anisotropy in easy axis phase

Another observation that also was predicted by the analytical solutions, is that for every direction of the magnetic field  $\vec{n}$  is stable in the  $xy$ -plane if the field is strong enough. This should be the case due to the already explained reasons that  $\vec{n}$  tries to be orthogonal to  $\vec{H}$ , the uniaxial anisotropy is overpowered by a strong field and the  $DMI$ -field drags  $\vec{n}$  in the  $xy$ -plane. This scans reproduced the behaviour from the previous ones and demonstrated the expected behaviour by the analytical method.

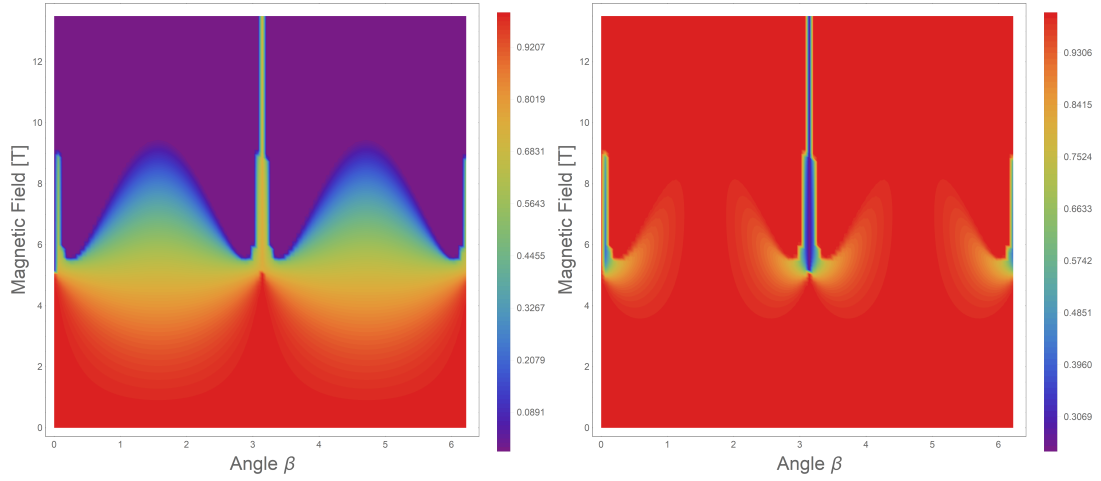


Figure 3.7.: Spin Hall magnetoresistance for different magnetic field strengths and directions in the  $xz$ -plane in the easy axis phase. The colourmap indicates the value for  $R_{xx}$  on the left and  $R_{yy}$  on the right.

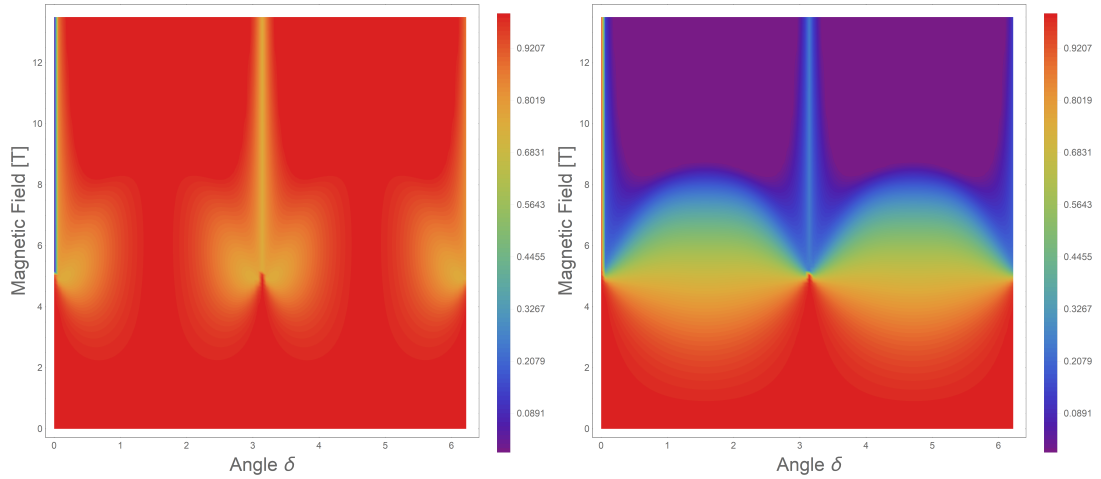


Figure 3.8.: Spin Hall magnetoresistance for different magnetic field strengths and directions in the  $yz$ -plane in the easy axis phase. The colourmap indicates the value for  $R_{xx}$  on the left and  $R_{yy}$  on the right.

### 3.4. Phase diagrams

Since we have learned about the behaviour of  $\vec{n}$  and produced testable results, we can now use this method to create a phase diagram for the magnetic states in hematite. The scans were changed a bit so that it now scans through two components of the field (e.g  $H_x$  and  $H_y$ ), while the third one is set to 0, instead of field strength and angle. The scans were done in 50 steps for each component of field from 0 T to 15 T. With the results from the scan we can plot the projection of  $\vec{n}$  into the xy-plane in dependence of the magnetic field. With the length of the projection of  $\vec{n}$  we can distinguish between three phases. In one phase  $\vec{n}$  is on the z- axis, and in another phase  $\vec{n}$  is perpendicular to the z-axis. Inbetween  $\vec{n}$  rotates from the z-axis into the xy-plane. The phases were distinguished by calculating  $n_x^2 + n_y^2$  for every data point and to compare them to 0 and 1 with a tolerance of 0.01.

In Fig. 3.9 we see again the expected behaviour of  $\vec{n}$  that we also obtained previously. We can also again obtain the effect of the *DMI*-field, that gives  $\vec{n}$  a certain preferred relation to  $\vec{H}$  in the xy-plane. The phase transition points were calculated in 2.5 for the simple case without  $H_{\perp}$  but for the small  $H_{\perp}$  they should still be valid.

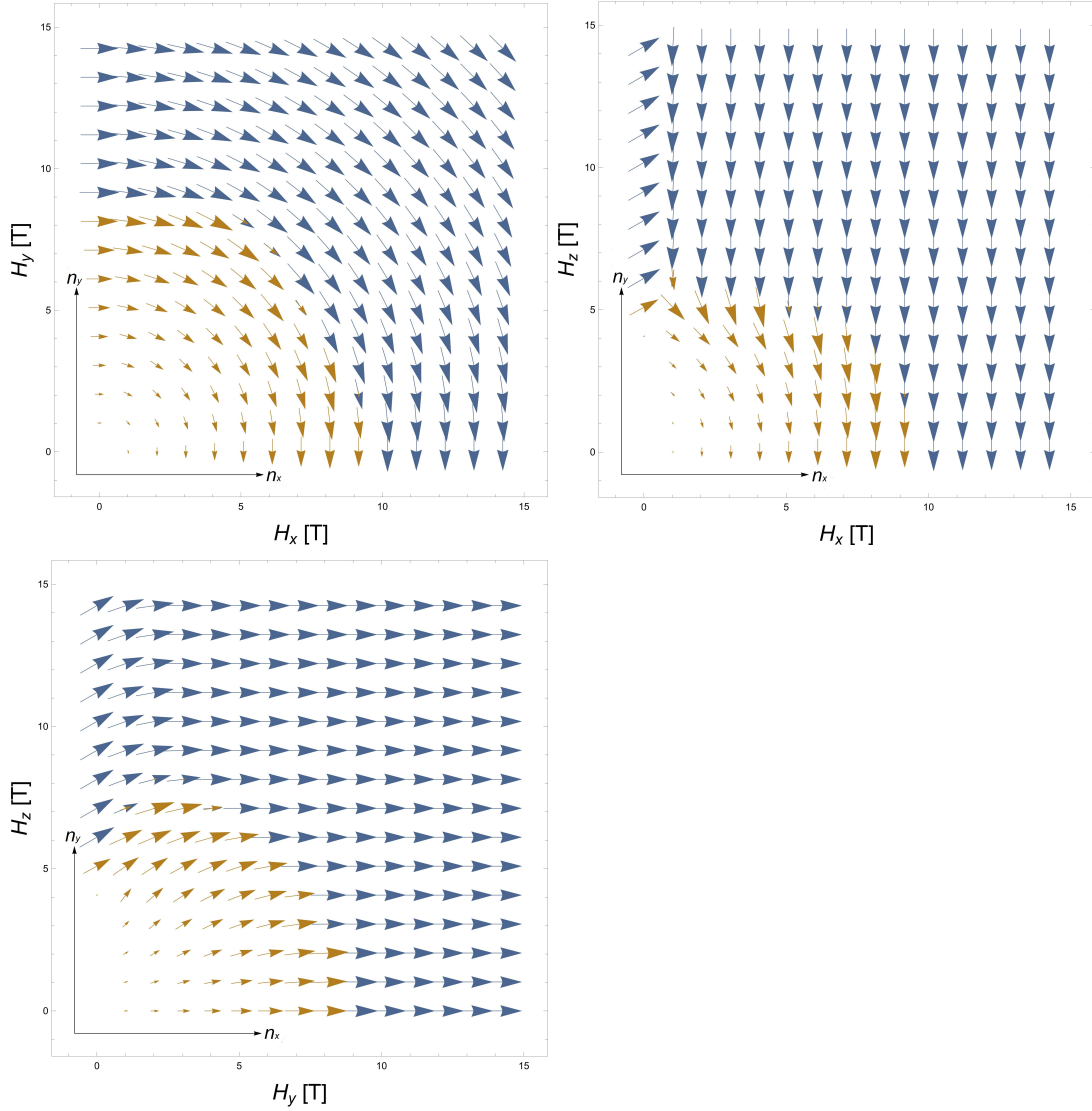


Figure 3.9.: Phase diagrams with the orientation of  $\vec{n}$  in the xy-plane for different magnetic fields. At the positions without an arrow we find the first phase with  $\vec{n} \parallel \hat{z}$  since the projection is zero. The second phase (brown) then occurs when  $\vec{n}$  rotates away from the z axis into the spin flop phase (blue), where the system is saturated and  $\vec{n}$  does not change by raising the field.

## 4. Numerical investigation of the anisotropy in easy plane phase

After analysing the easy axis phase, now it is interesting to test also the results from the easy plane phase. The used method is the same as in the previous section and all parameters were chosen equivalent except for  $\overline{H}_{2\parallel}$  which now is  $-24.09$  mT.

We expect as in the easy axis phase that in the  $\alpha$ -scan  $\vec{n}$  rotates away from the magnetic field by scanning through the angle, while in the  $\beta$ - and  $\delta$ -scan  $\vec{n}$  should be invariant under direction changes. If we scan through the field we would expect that  $\vec{n}$  is invariant since the stability of the analytical obtained states did not depend on the field strength. The may be only a small change for low fields, if  $\vec{n}$  is in an intermediate state between x- and y-axis for zero field. Then  $\vec{n}$  would probably rotate away from this state onto the axis where  $\vec{n} \perp \vec{H}$  while increasing the field. This should if it happens just cover a small range of the magnetic field.

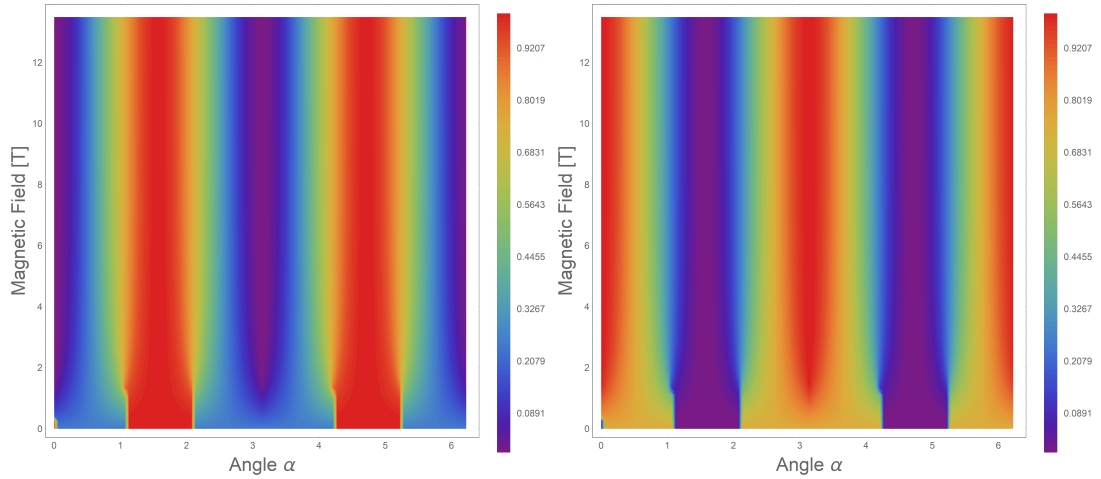


Figure 4.1.: Spin Hall magnetoresistance for different magnetic field strengths and directions in the xy-plane in the easy plane phase. The colourmap indicates the value for  $R_{xx}$  on the left and  $R_{yy}$  on the right.

---

4. Numerical investigation of the anisotropy in easy plane phase

---

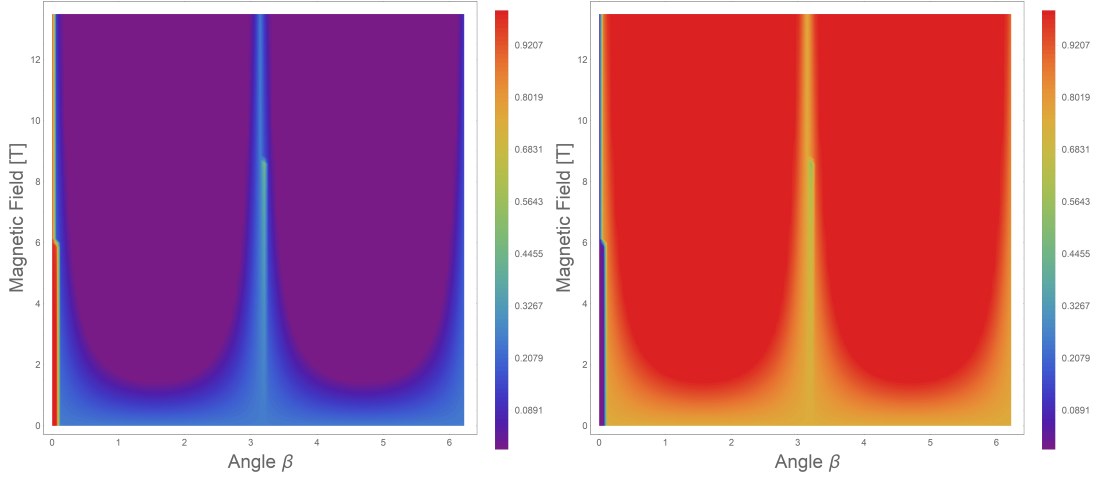


Figure 4.2.: Spin Hall magnetoresistance for different magnetic field strengths and directions in the  $xz$ -plane in the easy plane phase. The colourmap indicates the value for  $R_{xx}$  on the left and  $R_{yy}$  on the right.

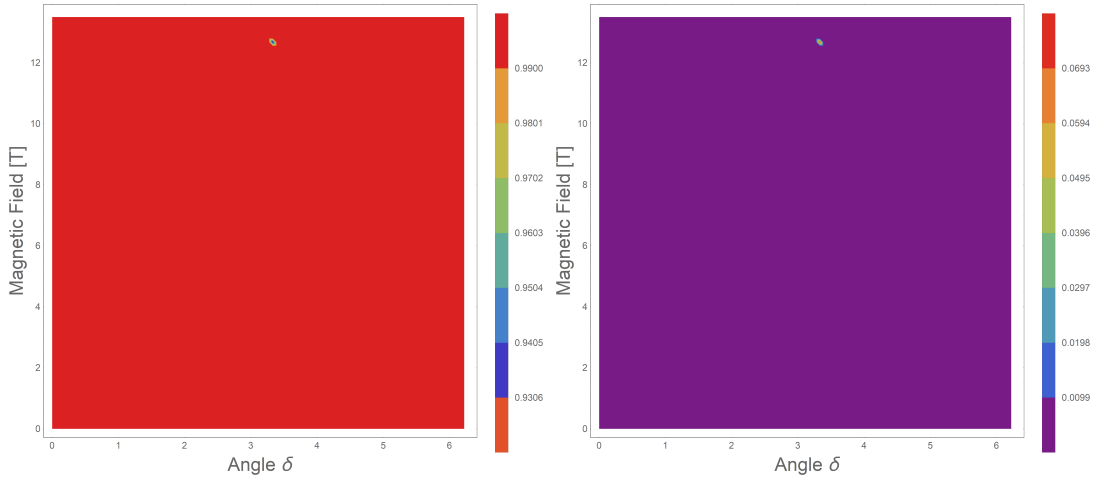


Figure 4.3.: Spin Hall magnetoresistance for different magnetic field strengths and directions in the  $yz$ -plane in the easy plane phase. The colourmap indicates the value for  $R_{xx}$  on the left and  $R_{yy}$  on the right.

In Fig. 4.1, 4.2 and 4.3 the two dimensional scans for the easy axis are shown. The one dimensional ones were put in the appendix. First of all we see again that we have a singularity if the field is applied along the easy axis. For the  $\beta$ -scan this stretches over the whole range of the external field while in the  $\delta$ -scan we only have one point at  $H = 12.7$  T that should not have the computed value. Also in the  $\delta$ -scan in Fig. A.7 we also see deviations from 0 in  $R_{yy}$  besides the place  $\delta = \pi$ . This may have

happened due to the same reason than the singularity at the easy axis but since the deviations are small they are negligible

We can see in Fig. 4.1 how  $\vec{n}$  rotates away from the field but is invariant under changes in the field strength. For the  $\beta$ -scan in Fig. 4.2 we see how  $\vec{n}$  rotates into the y-axis at low fields as predicted and is then invariant as expected. Also  $\vec{n}$  does not change with the angle. For the  $\delta$ -scan, we can see in Fig. 4.3 how  $\vec{n}$  is invariant parallel to the x-axis under changes of the field strength and direction. For all scans we see by looking at the values of both magnetoresistances together that  $\vec{n}$  is always in the xy-plane with a negligible deviation as it can be seen in Fig. A.6 with the plot for  $\cos\theta$ . There we see that  $\cos\theta$  has a deviation from 0 of the order of magnitude of  $10^{-7}$ . This was also predicted by the analytical calculations.

Since we only have found only one phase for each scan, drawing a phase diagram will be omitted here.

## 5. Conclusion

We did an analytical calculation to observe the behaviour of the Néel vector in hematite under an external magnetic field. We found out that  $\vec{n}$  normally is orientated on the easy axis in the easy axis phase for no field and then if the field is aligned on the easy axis instantly flips after the uniaxial anisotropy gets overpowered by the external field. If the field is not on the easy axis the Néel vector rotates out of the easy axis into a saturated state in the easy plane with rising field, while it depends on the orientation how "fast" the rotation goes. The closer the external field is to the easy plane the higher is the field where the saturation sets in. In the easy plane phase we observed that there is always a stable state for the Néel vector in the easy plane that gets not influenced by the external field. This observations all hold for the case where we did not consider in-plane anisotropy but since this anisotropy is small compared to the other internal fields, we did not expect a big change of the qualitative behaviour of the Néel vector by considering the in plane anisotropy.

We could verify the analytically obtained results for the easy axis phase with a numerical approach by simulating the dynamics of the Néel vector inside of hematite. The results did qualitatively match the analytical ones and also the discovered transition points into the spin flop phase, that could be predicted after choosing the internal fields, were reproduced. From the results that the numerical analysis method gave a phase diagram was created that distinguishes between a phase where the Néel vector is on the easy axis, a phase where it rotates away from this axis and the spin flop phase in the easy plane where the Néel vector is invariant if the field rises. Also for the easy plane phase the analytically obtained results could be verified. We showed that the Néel vector is invariant under changes in the magnetic field after at about 2 T in general and up to 5 T if the field is close to the easy axis. We could also show how the Néel vector aligns perpendicular to the magnetic field in and that it is always set in the easy plane.

During the numerical approach we found a singularity if the field was applied along the easy axis due to the low number of steps in the scan which was limited due to the technical resources.

The first task from now would be to do a more detailed scan with a shorter distance between the scanning steps to get rid of the singularities. Afterwards it would be meaningful to test the results from this work experimentally. Before the results could be used any further it would make sense to test them to demonstrate if the analysing methods did or did not work.

Under the assumption that the experiment would fit to the observed results it would be reasonable to see how the obtained results can be used in further research. Since we now know how the magnetic ordering behaves under a magnetic field in a

## 5. Conclusion

---

static case with fixed temperature the next question would be how the Néel vector behaves with under a dynamic Lagrangian and to investigate the differences we add a temperature gradient or change the temperature with time. From this, the new task would be to find out if the obtained informations can be used to write or read information on hematite or antiferromagnets in general and if this is possible to test the stability of the written information under external fields.

On a long range the task would be to find out if spin based information systems on antiferromagnets are possible and if so how effective these systems can be compared to recent information systems.

# A. Appendix

## A.1. Additional plots for the scans in the easy axis phase

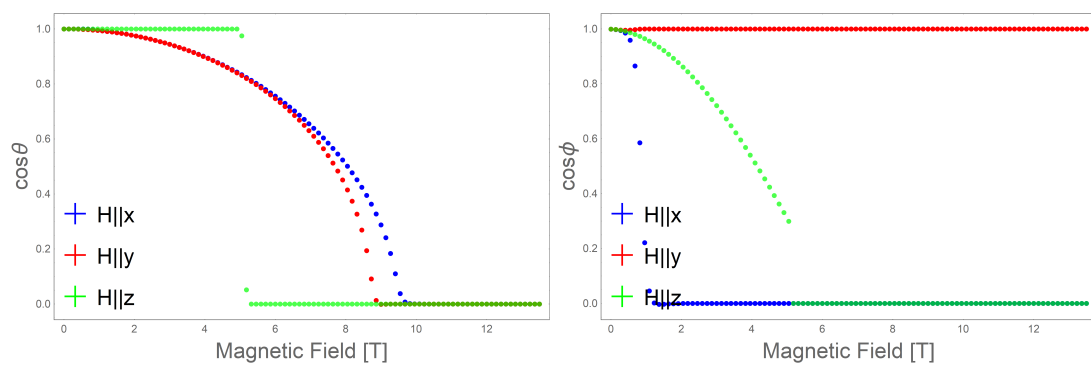


Figure A.1.: The orientation of  $\vec{n}$  described by  $\theta$  and  $\phi$  for the magnetic field aligned in a fixed direction in the easy axis phase.

A. Appendix

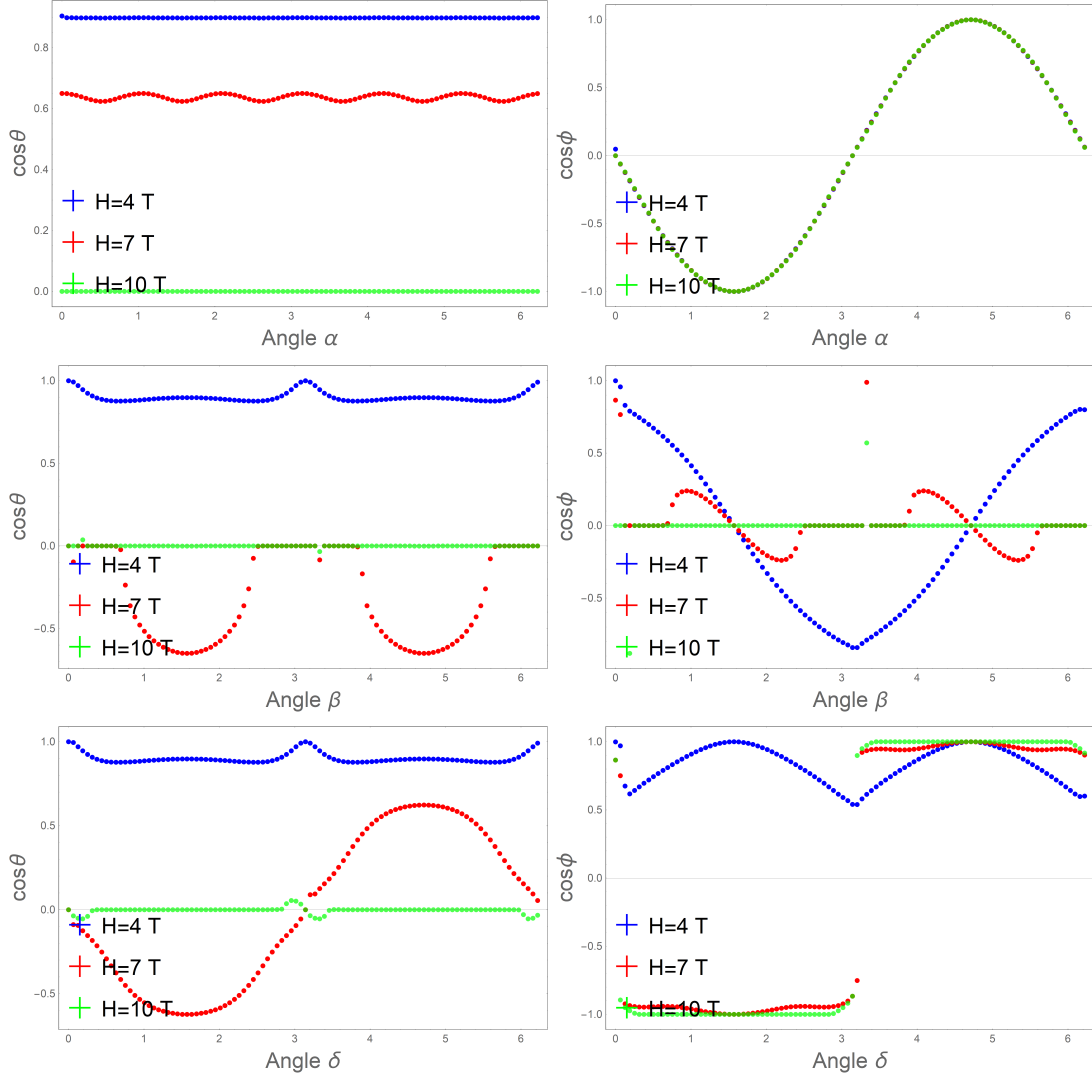


Figure A.2.: The orientation of  $\vec{n}$  described by  $\theta$  and  $\phi$  for the magnetic field rotation in different planes with fixed field strength in the easy axis phase.

## A. Appendix

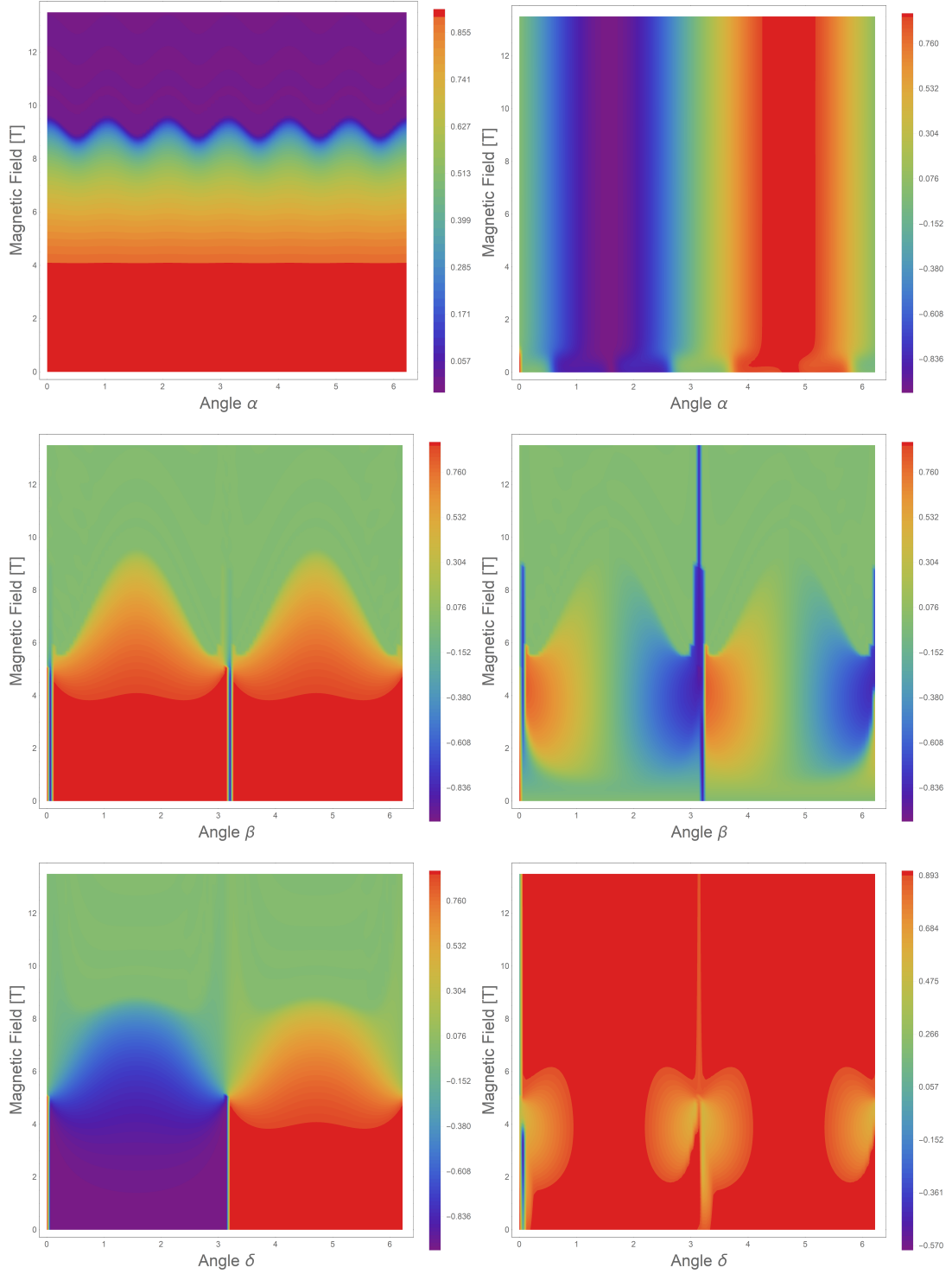


Figure A.3.: The orientation of  $\vec{n}$  described by  $\theta$  and  $\phi$  for the magnetic field rotation in different planes with variable field strength in the easy axis phase. The colourmap indicated the value of  $\cos \theta$  on the left and  $\cos \phi$  on the right.

## A.2. Additional plots for the scans in the easy plane phase

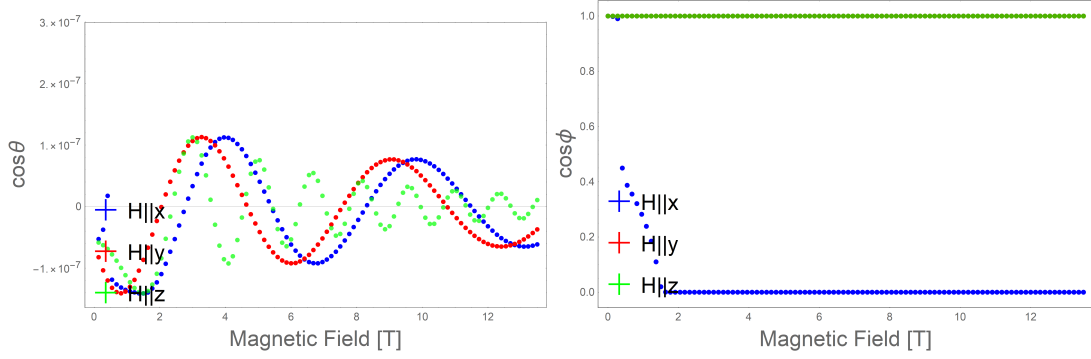


Figure A.4.: The orientation of  $\vec{n}$  described by  $\theta$  and  $\phi$  for the magnetic field aligned in a fixed direction in the easy plane phase.

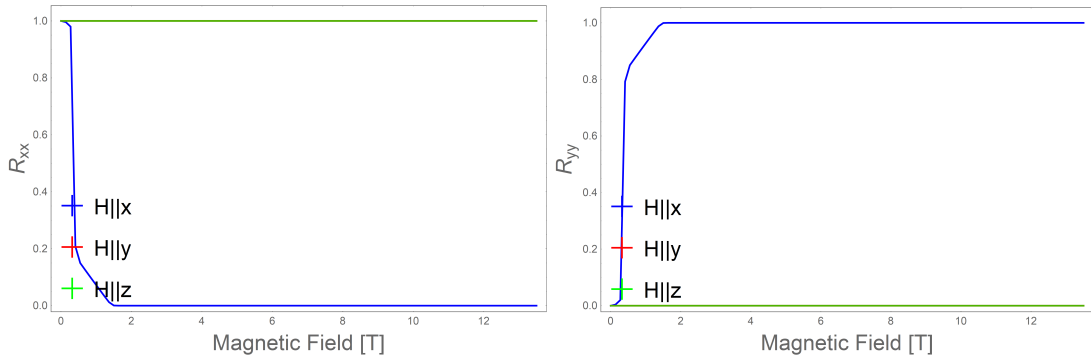


Figure A.5.: Spin Hall magnetoresistance for the magnetic field aligned in a fixed direction in the easy plane phase.

A. Appendix

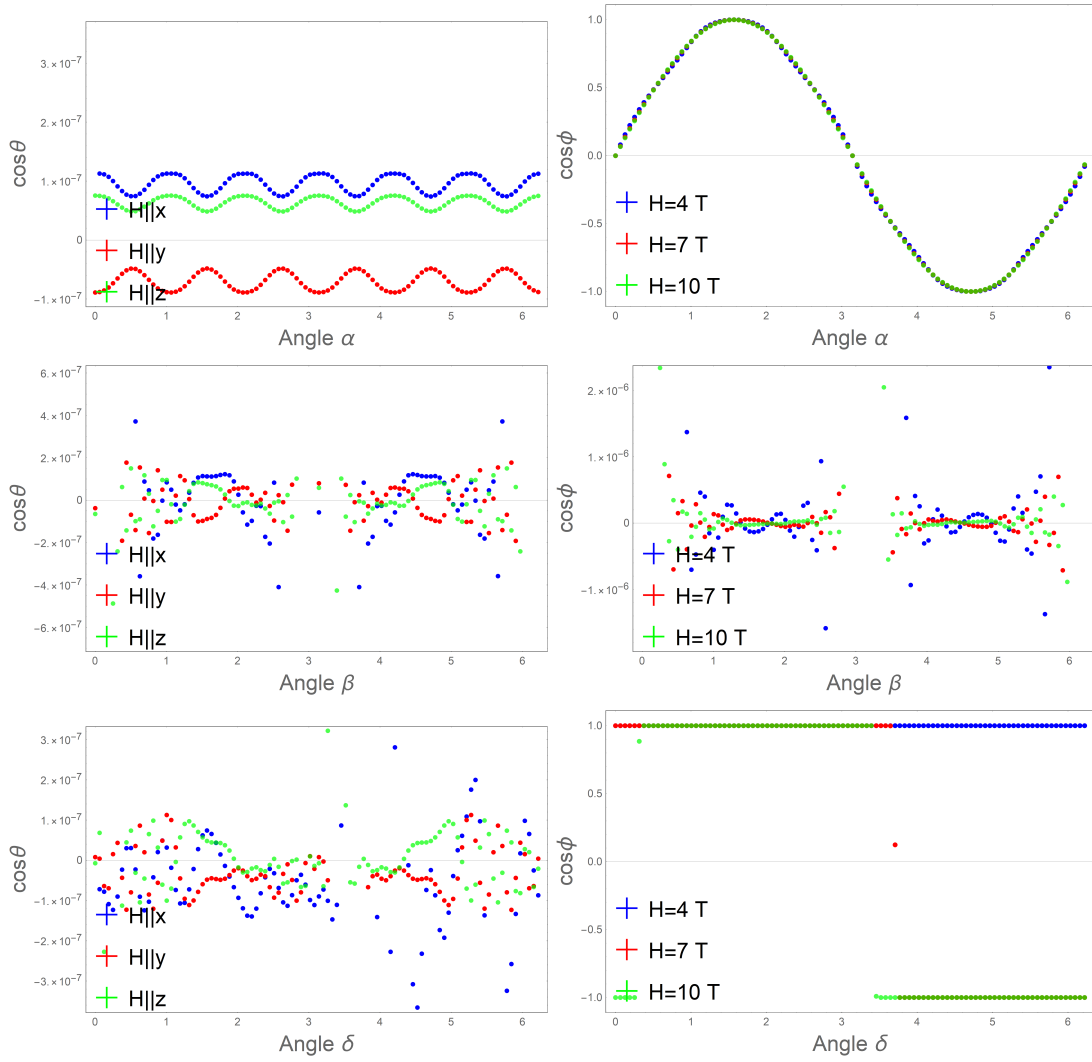


Figure A.6.: The orientation of  $\vec{n}$  described by  $\theta$  and  $\phi$  for the magnetic field rotation in different planes with fixed field strength in the easy plane phase.

A. Appendix

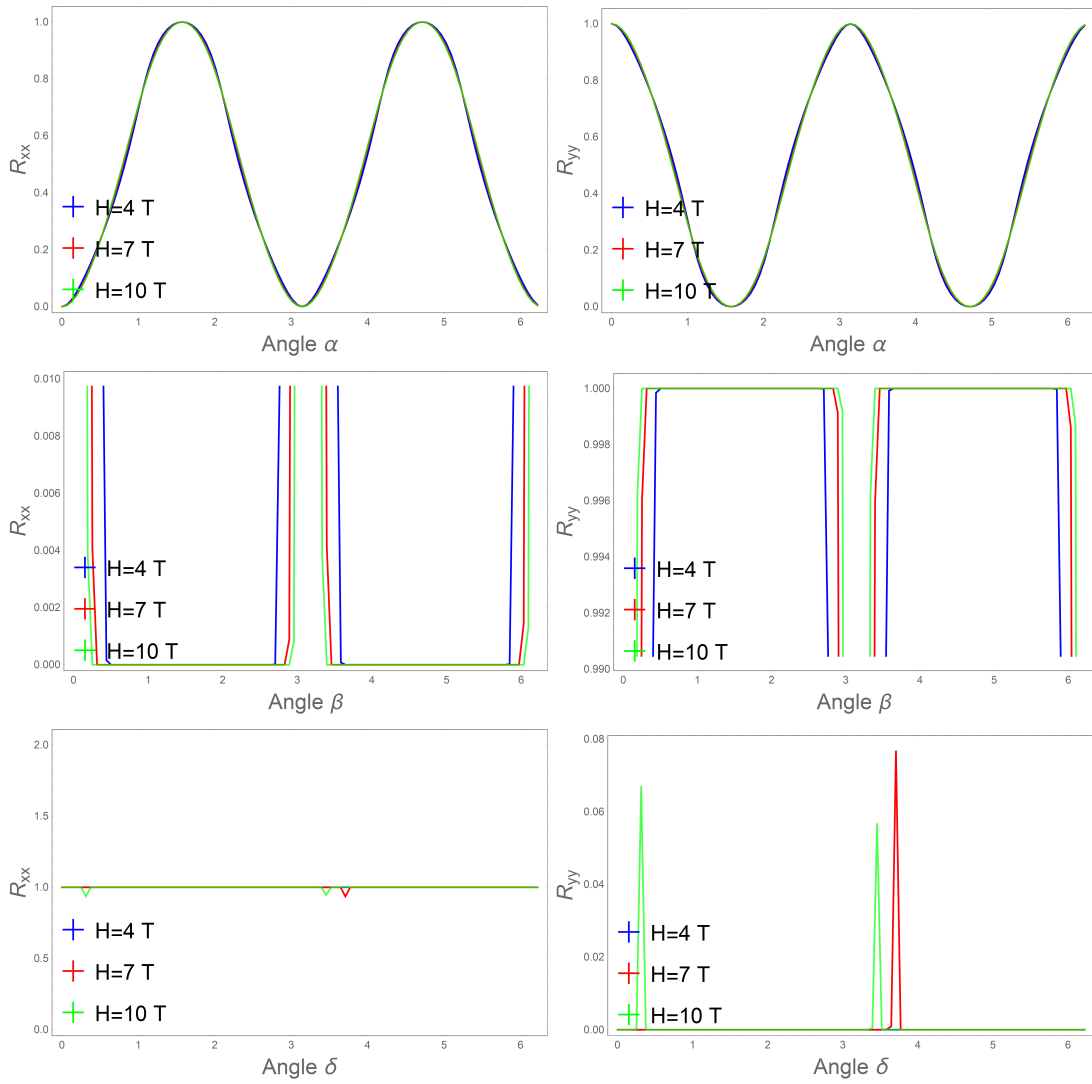


Figure A.7.: Spin Hall for the magnetic field rotation in different planes with fixed field strength in the easy plane phase.

A. Appendix

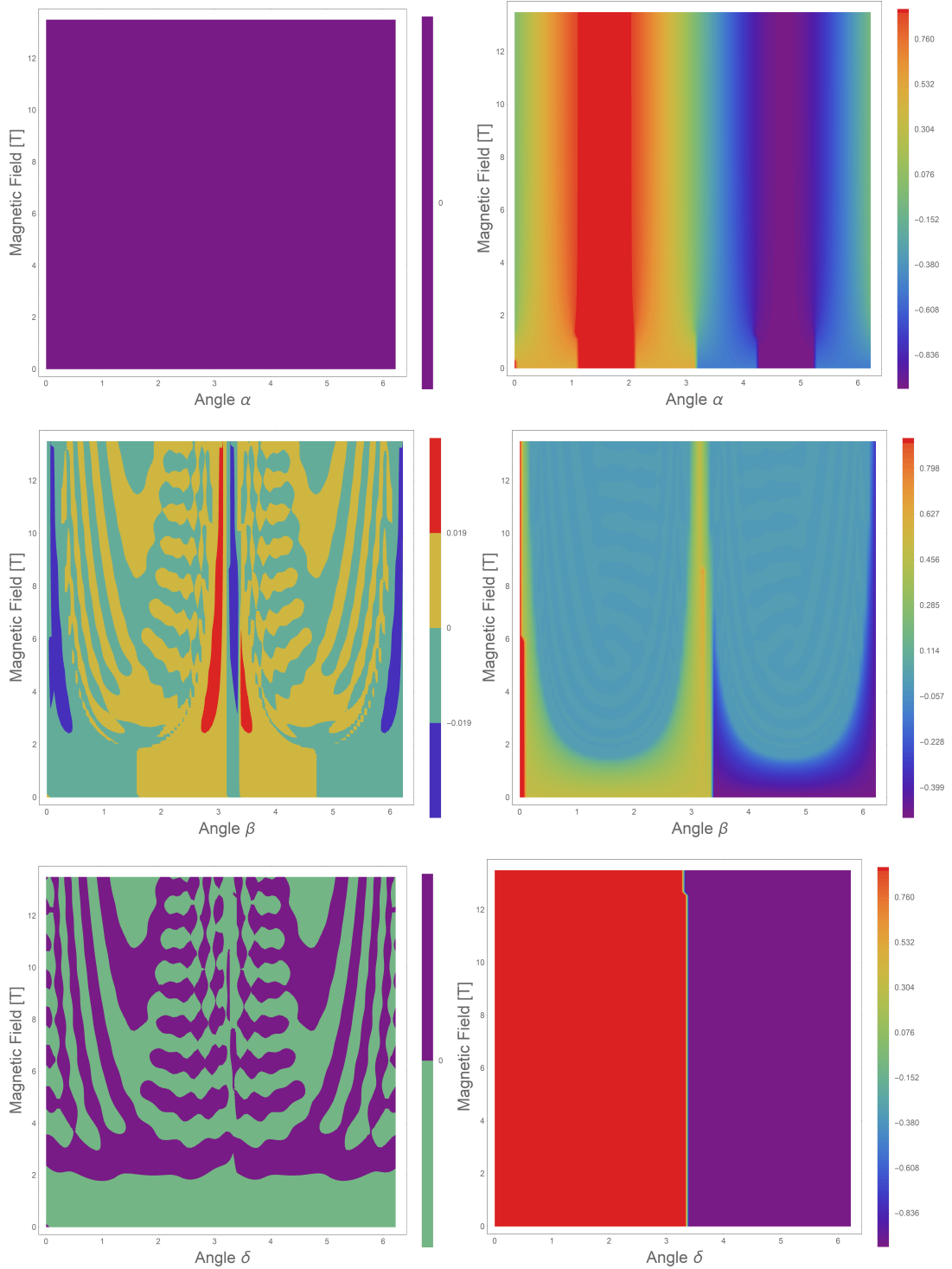


Figure A.8.: The orientation of  $\vec{n}$  described by  $\theta$  and  $\phi$  for the magnetic field rotation in different planes with variable field strength in the easy plane phase. The colourmap indicated the value of  $\cos\theta$  on the left and  $\cos\phi$  on the right.

## Bibliography

- [1] WHITE, Robert M. ; WHITE, Robert M. ; BAYNE, Bradford:  
*Quantum theory of magnetism*. Bd. 1.  
Springer, 1983
- [2] BOZORTH, Richard M.:  
Ferromagnetism.  
In: *Ferromagnetism*, by Richard M. Bozorth, pp. 992. ISBN 0-7803-1032-2.  
Wiley-VCH, August 1993. (1993)
- [3] JUNGWIRTH, T. ; MARTI, X. ; WADLEY, P. ; WUNDERLICH, J.:  
In: *Nature Nanotechnology* 11 (2016), 231–241 S.
- [4] GOMONAY, O ; JUNGWIRTH, T ; SINOVA, Jairo:  
Concepts of antiferromagnetic spintronics.  
In: *physica status solidi (RRL)–Rapid Research Letters* 11 (2017), Nr. 4, S.  
1700022
- [5] BODNAR, S Y. ; ŠMEJKAL, L ; TUREK, I ; JUNGWIRTH, T ; GOMONAY, O ;  
SINOVA, J ; SAPOZHNIK, AA ; ELMERS, H-J ; KLÄUI, M ; JOURDAN, M:  
Writing and reading antiferromagnetic Mn<sub>2</sub>Au by Néel spin-orbit torques and  
large anisotropic magnetoresistance.  
In: *Nature Communications* 9 (2018), Nr. 1, S. 348
- [6] NÉEL, M. LOUIS:  
Propriétés magnétiques des ferrites ; ferrimagnétisme et antiferromagnétisme.  
In: *Ann. Phys.* 12 (1948), Nr. 3, 137-198.  
<http://dx.doi.org/10.1051/anphys/194812030137>. –  
DOI 10.1051/anphys/194812030137
- [7] JUNGWIRTH, Tomas ; MARTI, X ; WADLEY, P ; WUNDERLICH, J:  
Antiferromagnetic spintronics.  
In: *Nature nanotechnology* 11 (2016), Nr. 3, S. 231
- [8] BØDKER, Franz ; HANSEN, Mikkel ; BENDER KOCH, Christian ; LEFMANN, Kim  
; MØRUP, Steen:  
Magnetic Properties of Hematite Nanoparticles.  
In: *Physical Review B* 61 (2000), 03, S. 6826–6838.  
<http://dx.doi.org/10.1103/PhysRevB.61.6826>. –  
DOI 10.1103/PhysRevB.61.6826
- [9] YAMAMOTO, Kei ; GOMONAY, Olena ; SINOVA, Jairo ; SCHWIETE, Georg:  
Spin transfer torques and spin-dependent transport in a metallic F/AF/N tun-  
neling junction.

- In: *Phys. Rev. B* 98 (2018), Jul, 014406.  
<http://dx.doi.org/10.1103/PhysRevB.98.014406>. –  
DOI 10.1103/PhysRevB.98.014406
- [10] UYEDA, Seiya ; FULLER, MD ; BELSHE, JC ; GIRDLER, RW:  
Anisotropy of magnetic susceptibility of rocks and minerals.  
In: *Journal of Geophysical Research* 68 (1963), Nr. 1, S. 279–291
- [11] BESSER, P. J. ; MORRISH, A. H. ; SEARLE, C. W.:  
Magnetocrystalline Anisotropy of Pure and Doped Hematite.  
In: *Phys. Rev.* 153 (1967), Jan, S. 632–640.  
<http://dx.doi.org/10.1103/PhysRev.153.632>. –  
DOI 10.1103/PhysRev.153.632
- [12] LEBRUN, Romain ; ROSS, Andrew ; GOMONAY, Olena ; BENDER, Scott ; BALDRATI, Lorenzo ; KRONAST, Florian ; QAIUMZADEH, Alireza ; SINOVA, Jairo ; BRATAAS, Arne ; DUINE, Rembert u. a.:  
Anisotropies and magnetic phase transitions in insulating antiferromagnets determined by a Spin-Hall magnetoresistance probe.  
In: *arXiv preprint arXiv:1901.01213* (2019)
- [13] MORIYA, Tôru:  
Anisotropic superexchange interaction and weak ferromagnetism.  
In: *Physical Review* 120 (1960), Nr. 1, S. 91
- [14] MIYAWAKI, Jun ; SUGA, Shigemasa ; FUJIWARA, Hidenori ; URASAKI, Masato ; IKENO, Hidekazu ; NIWA, Hideharu ; KIUCHI, Hisao ; HARADA, Yoshihisa:  
Dzyaloshinskii-Moriya interaction in  $\alpha$ -Fe<sub>2</sub>O<sub>3</sub> measured by magnetic circular dichroism in resonant inelastic soft x-ray scattering.  
In: *Physical Review B* 96 (2017), Nr. 21, S. 214420
- [15] ELLISTON, PR ; TROUP, GJ:  
Some antiferromagnetic resonance measurements in  $\alpha$ -Fe<sub>2</sub>O<sub>3</sub>.  
In: *Journal of Physics C: Solid State Physics* 1 (1968), Nr. 1, S. 169
- [16] BESSER, PJ ; MORRISH, AH ; SEARLE, CW:  
Magnetocrystalline anisotropy of pure and doped hematite.  
In: *Physical Review* 153 (1967), Nr. 2, S. 632
- [17] ÖZDEMİR, Özden ; DUNLOP, David J. ; BERQUO, Thelma S.:  
Morin transition in hematite: size dependence and thermal hysteresis.  
In: *Geochemistry, Geophysics, Geosystems* 9 (2008), Nr. 10
- [18] BOGDANOV, AN ; ZHURAVLEV, AV ; RÖSSLER, UK:  
Spin-flop transition in uniaxial antiferromagnets: Magnetic phases, reorientation effects, and multidomain states.  
In: *Physical Review B* 75 (2007), Nr. 9, S. 094425
- [19] CHEN, Yan-Ting ; TAKAHASHI, Saburo ; NAKAYAMA, Hiroyasu ; ALTHAMMER, Matthias ; GOENNENWEIN, Sebastian T. ; SAITOH, Eiji ; BAUER, Gerrit E.:  
Theory of spin Hall magnetoresistance.

*Bibliography*

---

- In: *Physical Review B* 87 (2013), Nr. 14, S. 144411
- [20] Ji, Y ; MIAO, J ; MENG, KK ; REN, ZY ; DONG, BW ; XU, XG ; WU, Y ; JIANG, Y:  
Spin Hall magnetoresistance in an antiferromagnetic magnetoelectric Cr<sub>2</sub>O<sub>3</sub>/heavy-metal W heterostructure.  
In: *Applied Physics Letters* 110 (2017), Nr. 26, S. 262401